

FACILITY FORM 502

N65 18448	
(ACCESSION NUMBER)	(THRU)
72	1
(PAGES)	(CODE)
057134	03
(NASA CR OR TRX OR AD NUMBER)	(CATEGORY)

Best available copy

**E**  
**S**

**ELECTRO-OPTICAL SYSTEMS, INC.,** Pasadena, California  
A Subsidiary of the XEROX Corporation

GPO PRICE \$ \_\_\_\_\_

OTS PRICE(S) \$ \_\_\_\_\_

Hard copy (HC) 3.00

Microfiche (MF) 75

Final Report, 1 November 1961 through 31 January 1963

FEASIBILITY STUDY TOWARD DEVELOPMENT OF  
RADIATION RESISTANT SOLAR CELL

Prepared for  
National Aeronautics and Space Administration  
Western Operations Office  
150 Pico Boulevard  
Santa Monica, California

Contract No. NAS7-92

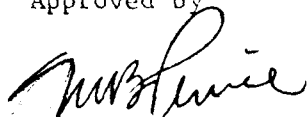
EOS Report 2080-Final

28 February 1963

Prepared by

M. Cheslow  
S. Kaye

Approved by



M. B. Prince, Manager  
SOLID STATE DIVISION

The applied research reported in this document has been made possible through support and sponsorship extended by National Aeronautics and Space Administration under Contract Number NAS7-92. It is published for technical information only, and does not necessarily represent recommendations or conclusions of the sponsoring agency.

ELECTRO-OPTICAL SYSTEMS, INC. - PASADENA, CALIFORNIA

ABSTRACT

18448

The results of a feasibility program to develop radiation resistant solar cells are described. An electric field in the base region which was produced by means of a graded base structure increased the collection efficiency of light produced carriers from the base region.

Comparative results of radiation damage tests with both 1 Mev electrons and 95 Mev protons are presented. The cells were found to be 20 times more radiation resistant than n-on-p cells having 1 ohm cm base region.

A complete theoretical discussion is given.

*AUTHOR*

#### ACKNOWLEDGMENTS

We would like to thank Dr. J. Denney and Mr. R. G. Downing of the Material Sciences Department of the Space Technology Laboratory for carrying out the electron and proton irradiation studies, and for the many helpful discussions which have taken place during this program.

We would also like to thank Mr. W. Scott and Mr. W. Cherry of the National Aeronautics and Space Administration for their guidance during the program; Mr. M. Rubinstein for the computer programing, and Mr. M. E. Koen for developing many of the processes used in the fabrication of the cells.

## TABLE OF CONTENTS

<u>Section</u>	<u>Page</u>
1. INTRODUCTION	1
2. CELL DESIGN AND FABRICATION	3
2.1 Cell Structure	3
2.2 Cell Fabrication, N-on-P Graded Base	5
2.3 Cell Fabrication P-on-N Graded Base	7
2.4 Control Cells	9
3. CELL CHARACTERISTICS	10
3.1 Base Impurity Profile	10
3.2 Lifetime, Capacitance and Series Resistance Measurements	14
3.3 Transit Time Experiments	16
3.4 Cell Efficiency Measurements	22
4. THEORY	24
4.1 Introduction	24
4.2 Continuity Equation	24
4.3 Absorption Properties and Field Effects	26
4.4 Carrier Distribution	28
4.5 Collection Efficiency	31
5. IRRADIATION EXPERIMENTS	37
5.1 Electron Irradiation	37
5.2 Proton Irradiation	47
5.3 NASA and STL Comparative Runs	47

<u>Section</u>	<u>Page</u>
6. COMPARISON OF THEORY VERSUS EXPERIMENT	51
7. CONFERENCES AND PUBLICATIONS	52
8. RECOMMENDATIONS FOR FUTURE WORK	54
REFERENCES	55
APPENDIX I - COMPUTER TECHNIQUES	

## LIST OF ILLUSTRATIONS

<u>Figure</u>		<u>Page</u>
1	Solar cell mask	4
2	Graded base solar cell	8
3	Conductivity vs distance from surface for boron diffusion into 25 $\mu$ cm P-type silicon	11
4	Conductivity vs distance from surface for high concentration of boron into 25 $\mu$ cm P-type silicon	11
5	Conductivity vs distance from surface of phosphorus diffusion into 150 $\mu$ cm N-type silicon	12
6	Conductivity vs distance from surface of phosphorus diffusion into 150 $\mu$ cm N-type silicon	12
7	Capacitance vs voltage for test junction	15
8	Circuit for measurement of device lifetime	15
9	Diagram of test setup	18
10	Diode test circuit	18
11	Test setup	19
12	Graded base cell illuminated from front	20
13	Graded base cell illuminated from back (unfiltered light)	20
14	Graded base cell illuminated from back (filtered light)	20
15	Control cell illuminated from front (unfiltered light)	21
16	Control cell illuminated from back (unfiltered light)	21
17	Photon spectra for space sunlight and 2800 $^{\circ}$ K tungsten light	27
18	Absorption of photons in silicon-differential spectra	27
19	Number of source photons absorbed above depth X: silicon	27

# LIST OF ILLUSTRATIONS (cont)

<u>Figure</u>		<u>Page</u>
20	Field in base region as a function of distance from the junction	29
21	Electron mobility vs impurity concentration in silicon	29
22	Electron mobility in graded base solar cell	29
23	Excess carrier distribution ( $E = 0$ )	30
24	Excess carrier distribution for $L = 100$ microns	30
25	Collection efficiency from infinite base region vs diffusion length and field strength in sunlight	33
26	Collection efficiency in $2800^{\circ}\text{K}$ tungsten light from infinite base region	33
27	Collection efficiency for finite base in sunlight vs electric field strength	34
28	Diffusion length vs flux of 1 mev electrons: P-type silicon	34
29	Total collection efficiency in sunlight vs 1 mev electron flux and internal field strength	35
30	Total collection efficiency in $2800^{\circ}\text{K}$ tungsten vs 1 mev electron flux and internal field strength	35
31	Theoretical short circuit current density vs 1 mev electron flux in tungsten light	35
32	Short circuit current density as a function of 1 mev electron flux	39
33	Short circuit current density as a function of 1 mev electron flux	39
32	Short circuit current density as a function of 1 mev electron flux	41
34	Short circuit current density as a function of 1 mev electron flux	41
32	Short circuit current density as a function of 1 mev electron flux	43
35	Short circuit current density as a function of 1 mev electron flux	43
32	Short circuit current density as a function of 1 mev electron flux	45



# LIST OF ILLUSTRATIONS (cont)

<u>Figure</u>		<u>Page</u>
36	Short circuit current density as a function of 1 mev electron flux	45
37	Short circuit current density as a function of 1 mev electron flux	48
38	Integrated proton flux/cm <sup>2</sup> (95.5 mev)	48
39	Comparative degradation of various N-on-P solar cells irradiated at NRL by NASA	50
40	Comparative degradation of various N-on-P solar cells irradiated at STL (based on a figure of R.G. Downing)	50

## 1. INTRODUCTION

This report discusses the results of a fifteen month program carried out by Electro-Optical Systems, Inc., to determine the feasibility of fabricating radiation resistant solar cells in silicon. The principal use for solar cell power supplies is to be found in space vehicles, and it has been established that those vehicles which are in earth orbits are subjected to high energy particle bombardment consisting of protons and electrons. The effect of this bombardment on the cells is to reduce their conversion efficiency. This loss of efficiency is primarily due to a degradation of lifetime in the base region of the cell caused by the particle bombardment.

Electro-Optical Systems, Inc., accordingly proposed the graded base concept as a method of overcoming this degradation. In this cell design, an electric field is introduced into the base region of the cell. The effect of this field is to increase the effective velocity flow of light-generated minority carriers towards the p-n junction. By use of this field-assisted flow the probability of recombination of the minority carriers is considerably reduced and hence the effect of the particle-induced decrease in lifetime is lessened. The electric field in the base region is produced by means of a controlled gradient of impurities within the region.

During the program, graded base cells were fabricated, using diffusion to produce the impurity gradient within the base region of the cell. The cells fabricated had initial efficiencies, when measured in sunlight, of as high as 11 percent. A number of these cells were irradiated with either 1 Mev electron or 94 Mev protons.

It was found that the short circuit current of graded base cells underwent less degradation than that of any cell produced with a uniform distribution of dopant impurities in the base.

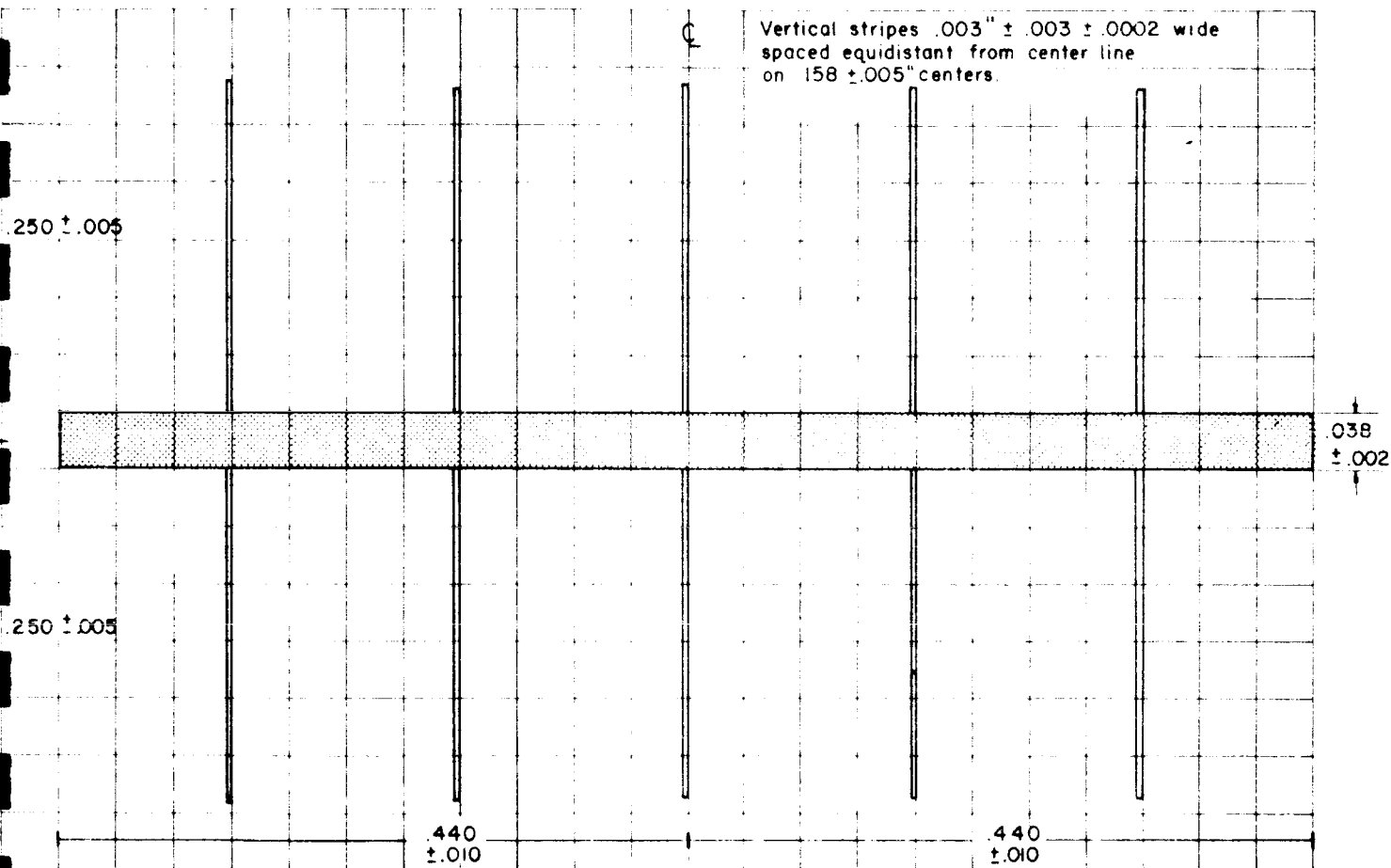
These experimental results, which were obtained at Space Technology Laboratories and at the Naval Research Labs for NASA, confirmed the detailed theoretical predictions which had also been made during the course of this program.

## 2. CELL DESIGN AND FABRICATION

### 2.1 Cell Structure

Preliminary design considerations (Ref. 1) indicated that it would be possible to obtain fields of between 20 and 40 volts/cm in silicon by the use of a diffusion process to form the graded base region, provided that the thickness of the region was restricted to 4 to 4-1/2 mils and that the starting material had a carrier density of  $2 \times 10^{14}$  or less. It was also decided initially that the cells should be of the n-on-p type since earlier work (Ref. 2) had shown that these cells were considerably more radiation resistant than were the p-on-n devices. Thus, the starting material was selected to be 25 ohm cm p-type silicon.

In order to obtain meaningful results, it was realized that it was necessary to prepare cells of the highest possible conversion efficiency, and so in order to minimize the series resistance of the cells a gridded structure was adopted. Figure 1 shows the design of the mask that was employed in order to obtain the gridded structure for the cell front contact. Cells having dimensions of both 1 x 1 and 1 x 2 cm were fabricated. The choice of which cell size was employed by an particular experiment was merely a matter of convenience. In addition to fabricating graded base n-on-p cells, some graded base p-on-n cells were also fabricated and tested. In addition, n-on-p control cells, having a uniform resistivity in the base region, were fabricated. The following sections discuss the fabrication techniques employed for the manufacture of these various types of cells.



NOTE: SHADED AREAS and VERTICAL STRIPES - BLACK

FIG. 1 SOLAR CELL MASK

## 2.2 Cell Fabrication, N-on-P Graded Base

The fabrication of cells consists of two diffusion steps, the first of which provides the graded impurity region for the base and the second of which produces the p-n junction. Contacts are then made to both the p and n regions of the cell; contact to the n region is a gridded structure in order to reduce the series resistance. The cell is coated with an anti-reflection coating of silicon monoxide which is applied by evaporation.

Table I shows the major process steps in some more detail. Prior to the first diffusion, boron is applied by painting on a suspension of  $B_2O_3$  in a solvent. After the solvent has dried, the slices are diffused at  $1250^\circ C$  for 100 hours in an air atmosphere. At the end of this period the furnace is turned off and allowed to cool to  $750^\circ C$  at which temperature the slices are withdrawn from the furnace. The slices are then mounted on lapping jigs and lapped in a Lap-master machine on one side only, to a thickness of 6.5 to 7 mils. The slices are then mounted so that the unlapped side is protected by wax and etched in a polishing etch to a final thickness of 4 to 4.1 mils. After being demounted and cleaned, the slices are then diffused with phosphorous to form the p-n junction. This diffusion takes place at a temperature of  $930^\circ C$  for 30 minutes in an atmosphere of dry nitrogen. The diffusion source is dry  $P_2O_5$  which is held in a quartz boat at a temperature of approximately  $300^\circ C$ . At the end of this 30 minute period the slices are withdrawn into a second furnace, which is then turned off and allowed to cool to  $750^\circ C$ , at which point the slices are withdrawn. The back or lapped surface of the slice is now given a light lap by hand to remove .5 to 1 micron of material, thus removing the diffused n-type region from the back of the cell.

TABLE I

1.	Clean Slices
2.	Paint on Boron
3.	Deep Diffusion
4.	Lap
5.	Etch
6.	Clean
7.	Diffuse Junction
8.	Hand Lap Back
9.	Mask
10.	Plate
11.	Cut
12.	Etch
13.	Solder Dip
14.	Anti-Reflection Coat

Photoresist is then applied to the front surface of the cell and exposed through the grid pattern mask and developed. The back of the cell and the unmasked portions of the front of the cell are then plated with a nickel-gold mixture, using an electroless process followed by an electrolytic plating of silver. The cells are then mounted for ultrasonic cutting and depending on the size of the piece involved, are cut either to 1 x 1 or 1 x 2 cm rectangular blanks. After being cleaned, the cells are then mounted for a junction clean-up etch in such a way that both the front and back surfaces of the cells are protected, leaving the edge to be attacked by a nitric hydrofluoric acid mix which removes the damaged material around the periphery of the cell. The cells are then solder dipped in a 60/40 solder at approximately 200°C and the front surface of the cell is then given an anti-reflection coating of silicon monoxide by vacuum evaporation.

The n-type diffusion is evaluated by measurements of sheet resistance and junction depth. Sheet resistance values run typically between 16 and 20 ohms per square, and junction depth is  $.45 \pm .05$  micron. Figure 2 shows a photograph of the completed cell.

### 2.3 Cell Fabrication P-on-N Graded Base

In order to obtain additional check of the applicability of the graded base concept to the improvement of solar cell radiation resistance, Mr. W. Cherry suggested that we fabricate p-on-n cells containing a graded base region. The fabrication techniques employed were essentially the same as those described in the previous section for the n-on-p cells with the exception of the diffusion procedures. The starting material was 15 ohm centimeter n-type silicon. The graded base region was produced by pre-depositing phosphorus onto the slices. A  $P_2O_5$  source was held at 300°C and the slices were held at a temperature of 1050°C for a period of 30 minutes.



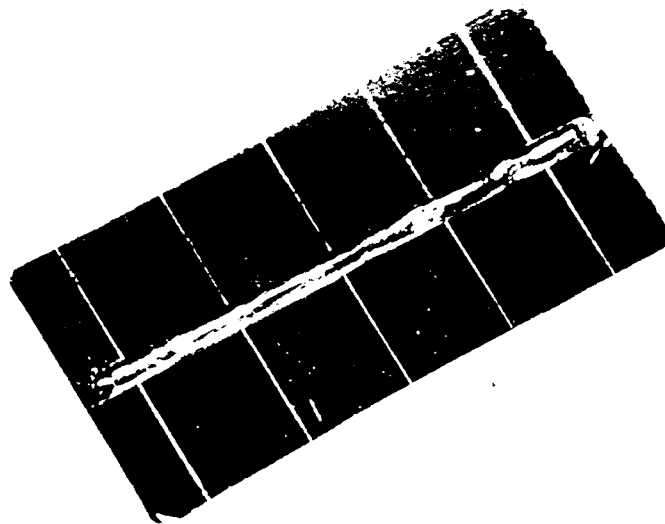


FIG. 2 GRADED BASE SOLAR CELL

The dopant was carried to the slices in a stream of dry nitrogen. The pre-deposited layer was then driven in by diffusion at a temperature of 1250°C for 100 hours. After lapping and etching the slices to a thickness of 4 mils, the p-type region was produced by carrying out the junction diffusion at a temperature of 1050°C for 12 minutes using a  $B_2O_3$  as a source. Subsequent processing was identical to that described in the previous section for n-on-p type cells.

#### 2.4 Control Cells

N-on-p control cells were fabricated using the same starting material which had been used for the graded base cells. Instead of performing a long diffusion to produce a graded base region, a short pre-deposition of  $B_2O_3$  was carried out in order to provide a p+ back surface so that a low resistance ohmic contact could be obtained to the back of the cell. With this exception, other processing was identical to that for the graded base cells. Two types of control cells were fabricated, having thicknesses of 4 mils and 12 mils, respectively.

### 3. CELL CHARACTERISTICS

#### 3.1 Base Impurity Profile

The impurity distribution in the base region of the cell was determined by the use of the following technique.

After the deep base diffusion, a sample slice from the run had one side removed by lapping and etching so that the slice thickness remaining was approximately 5 mils. The slice was then mounted with the etched face protected and the sheet resistance was measured using a four point probe on the back surface. 0.2 mils was then removed from the back surface and the sheet resistance measured again. These steps were repeated until the sheet resistance was too high for reliable measurements to be obtained.

The conductivity of the nth layer  $\sigma_n$  is then given by

$$\sigma_n = \left[ \frac{1}{R_{s(n)}} - \frac{1}{R_{s(n+1)}} \right] \frac{1}{X_n} \quad (1)$$

Where  $R_{s(n)}$  and  $R_{s(n+1)}$  are the sheet resistances before and after the removal of the nth layer and  $X_n$  is the thickness removed. The results of such measurements on typical cells are shown in Figs. 3 - 6. Figure 3 shows the results obtained using the normal boron paint-on technique which has been described for p-type base diffusions. It will be seen that the surface concentration is approximately  $3 \times 10^{19} \text{ cm}^{-3}$ . This result is typical of those obtained on a number of different runs. An attempt was made to determine the effects of increased boron concentration.

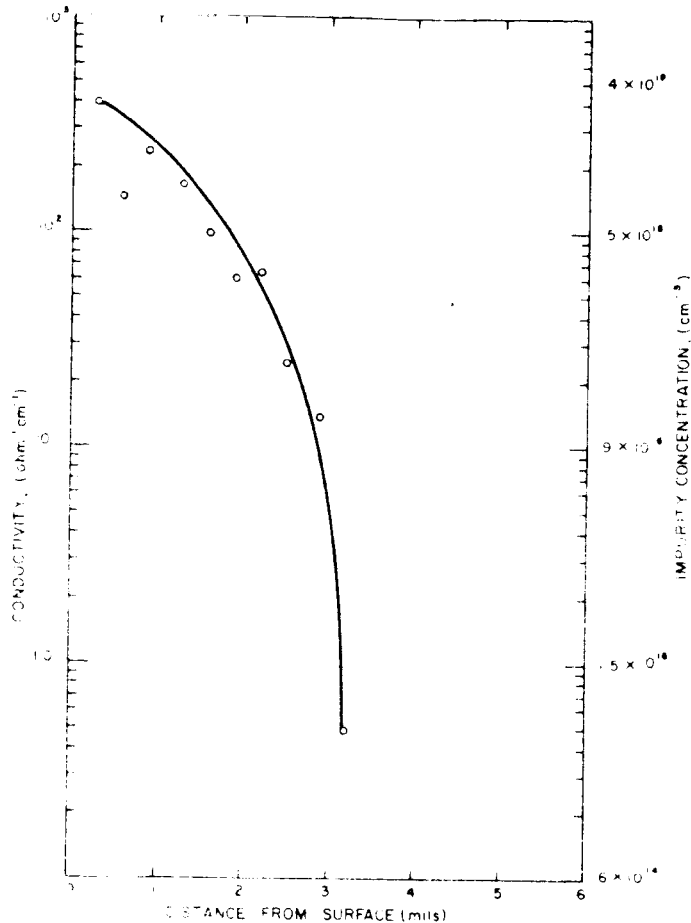
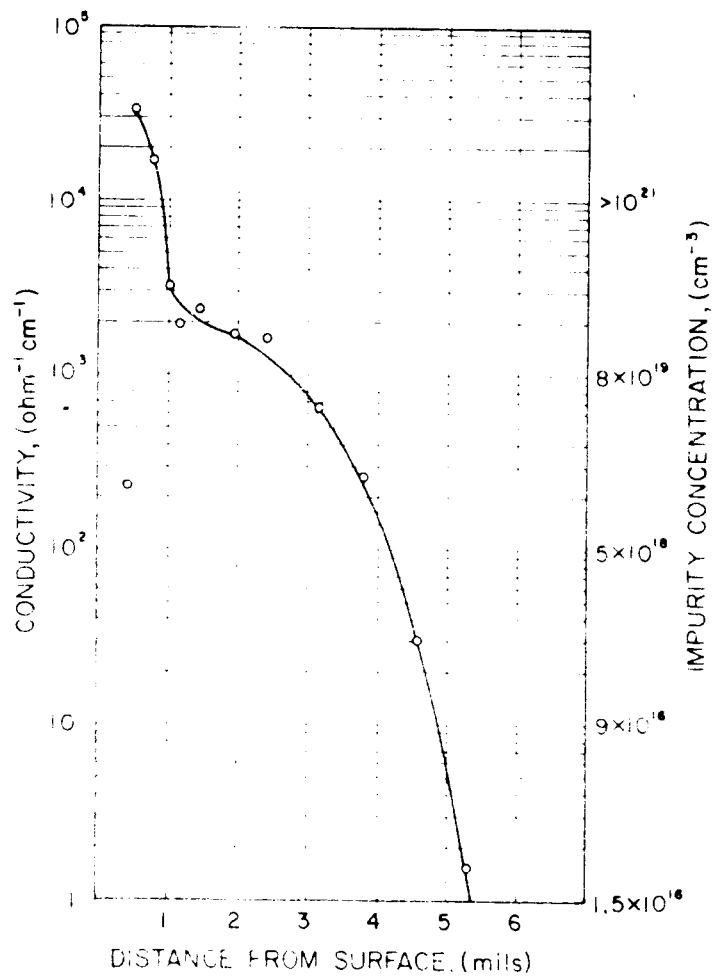


FIG. 3  
CONDUCTIVITY VS. DISTANCE FROM  
SURFACE FOR BORON DIFFUSION  
INTO 25  $\Omega$ cm P-TYPE SILICON

FIG. 4  
CONDUCTIVITY VS. DISTANCE FROM  
SURFACE FOR HIGH CONCENTRATIONS  
OF BORON INTO 25  $\Omega$ cm P-TYPE  
SILICON



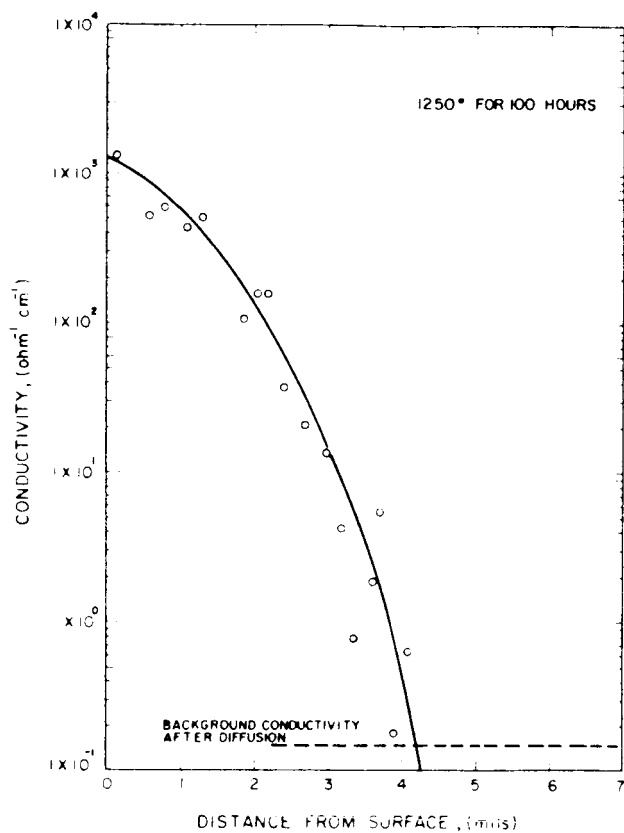


FIG. 5  
CONDUCTIVITY VS DISTANCE FROM  
SURFACE OF PHOSPHORUS DIFFUSION  
INTO 15Ω cm N-TYPE SILICON

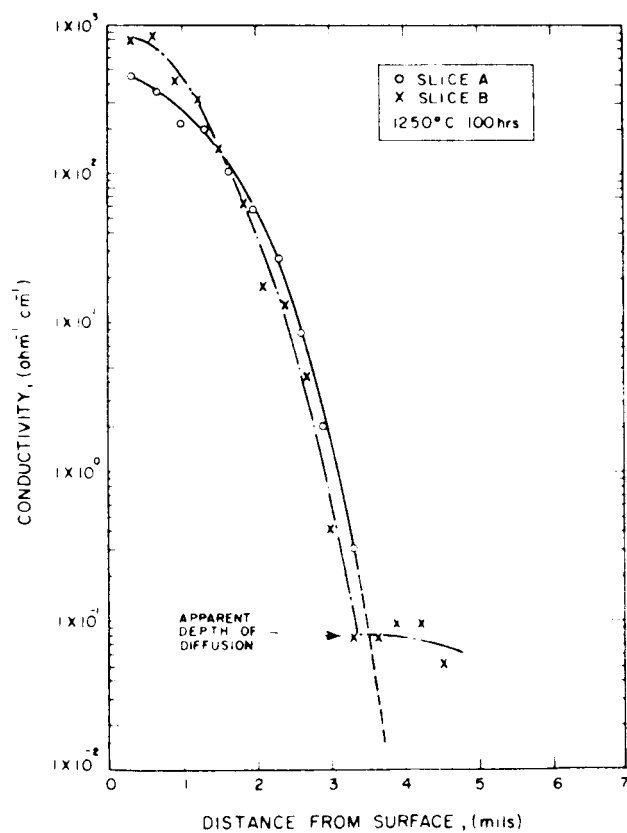


FIG. 6  
CONDUCTIVITY VS DISTANCE FROM  
SURFACE OF PHOSPHORUS DIFFUSION  
INTO 15Ω cm N-TYPE SILICON

The higher concentration was obtained by increasing the concentration of  $B_2O_3$  in the paint which is applied to the surface as the dopant prior to diffusion. Figure 4 shows the results of the impurity profile taken after such a diffusion. It will be seen that the surface concentration has increased by approximately an order of magnitude. It is not possible to tell whether the apparent point of inflection in the curve really exists or is due to difficulties of measurement.

It was not possible to fabricate cells from this more heavily doped material due to the fact that the very high concentration of boron caused considerable crystalline strain, and it was not possible to obtain smooth etched surfaces on the slices which had been subjected to this diffusion treatment.

From results shown in Figs 3 and 4 the electric field in the base region of the cell was calculated. Due to the uncertainties in the measurements, this calculation was at best an approximate estimate, and showed that in the case of the higher doped cell, an increase in the average electric field in the base region by at most 20 percent was obtained. Since this is a marginal increase, it was decided not to pursue these experiments further.

Figures 5 and 6 show similar curves obtained for phosphorus diffusion into n-type material. This material was used for the fabrication of p-on-n graded base cells.

### 3.2 Lifetime, Capacitance and Series Resistance Measurements

Early in the program it was decided to make both lifetime and capacitance measurements on fabricated cells in order to determine the resistivity of the base region immediately adjacent to the junction and the effective lifetime of the material adjacent to the junction. It was not possible to make these measurements on complete  $1 \text{ cm}^2$  area cells due to the large junction capacitances and leakages that are involved. Accordingly two samples were taken and mesas were etched on these samples in order to obtain junctions having areas of one to two  $\text{mm}^2$ . The capacitance of each of these junctions was measured as a function of the reverse bias voltage applied in the range of 2 to 10 volts, and was found to follow the  $V^{-1/2}$  law, as shown in Fig. 7 thus indicating an abrupt junction.

From this measurement and the measurement of the junction area, it was possible to deduce the resistivity of the base material adjacent to the junction and this was found to be 24 ohm cm. It was thus concluded that the diffusion processes were not changing the resistivity of the starting material in those regions sufficiently far from the surface that the impurities were not penetrating into them.

In addition to the capacitance measurements which were made on these mesas, lifetime measurements were also carried out using the junction injection method described in Ref. 3. The circuit used for these measurements is shown in Fig. 8. The results obtained, applying the theory as given in the reference, were 2 microseconds and 6 microseconds respectively. It is not clear, however, what the effect of the graded base region has been on the results obtained by this method of measurement so that these results must be treated with some caution.

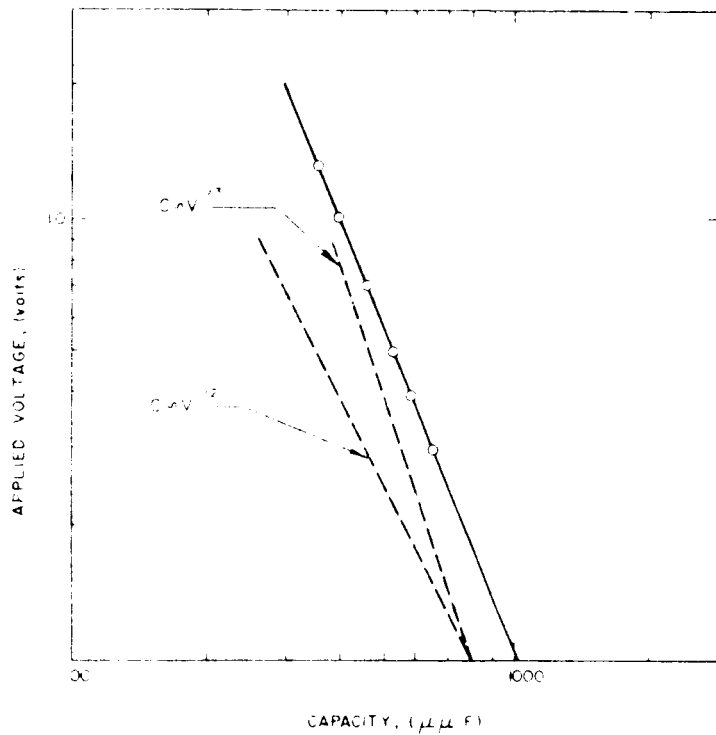


FIG. 7  
CAPACITANCE VS VOLTAGE FOR  
TEST JUNCTION

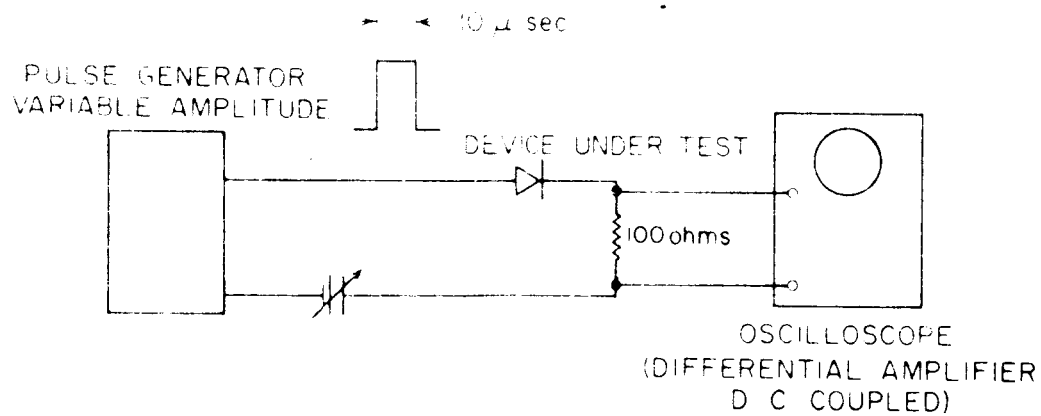


FIG. 8 CIRCUIT FOR MEASUREMENT OF  
DEVICE LIFETIME



The series resistance of two 10 to 11 percent cells was estimated using one of the methods described by Rauschenbach and Wolf (Ref.4). This method involves locating a point on each of the V-I curves taken at various light levels at a fixed current difference from the short circuit condition. When these points are joined by a straight line the reciprocal of the slope of the line gives the series resistance. In both cases the measured value of series resistance was approximately two ohms. Of these two ohms, one ohm can be accounted for by the resistance of the thin diffused n-type layer. The sheet resistance of the plated contact was measured using a four point probe and was found to be 0.05 ohms per square. The longitudinal resistance of the front contact stripe was calculated and was found to be one ohm. Since, when the cells are tested, contact is usually made with a point at one extremity of the stripe, this therefore counts for one ohm of the series resistance. Accordingly, the plating thickness has been increased on cells subsequently fabricated.

### 3.3 Transit Time Experiments

An experiment was carried out designed to measure the transit time of carriers injected into the back of a cell. It was expected that by this means it would be possible to verify the existence of an electric field in the base region of the cell driving the injected minority carriers towards the junction. If the case of a  $\delta$  function of injected carriers is considered, it can be shown that the transit time  $t$  for the injected carriers to move a distance  $W$  is given by Eq.(2) (Ref. 5 ).

$$t = \frac{W^2}{4D} \quad (2)$$

where

$D$  is the diffusion coefficient of the injected carriers.

For electrons in a layer of p-type silicon 100 microns thick, this transit time is 2.6 microseconds. Since it is expected that the electric field introduced into the base region by the diffusion of impurities will reduce the transit time to 1 microsecond or less. (Ref. 1). It should be possible to distinguish between the field and non-field case by injecting carriers into the back of the cell and measuring the time required for them to arrive at the junction. The method used of injecting the carriers was to use photo-injection, and the setup is shown diagrammatically in Fig. 9. The cell under test was illuminated with a pulse of light, 1 microsecond long using a Kerr cell shutter as a means of producing the pulse. The device to be tested was prepared by taking a portion of a solar cell and etching a mesa approximately 2 mm in diameter on the front surface of the cell. Pressure contacts were made to this diode structure which could be illuminated either from the front or the back by reversing the diode in its holder. The measurement circuit is shown in Fig. 10. Due to the fact that the Kerr cell required 35 KV pulses to operate it, it was necessary to shield the complete circuit shown in Fig. 10 very carefully in order to prevent electro static pickup. Figure 11 is a photograph of the complete test setup in use.

Figures 12 through 16 are photographs of the oscilloscope traces made under various conditions of illumination of both graded base and control cells. Figures 12, 13 and 14 were obtained on a mesa etched from a portion of a graded base cell. Figure 12 shows the trace obtained when the cell was illuminated with 1 microsecond pulse of light on its front surface. Figures 13 and 14 show the results obtained with the same specimen when it was illuminated from the back. In Fig. 13 no filter was used, but in Fig. 14 a Corning CS4-97 filter, which is a blue-green filter having zero transmission in the near infrared, was interposed in the optical path. It will be noticed that there is no difference in the general characteristic of the curve between Fig. 13 and 14.

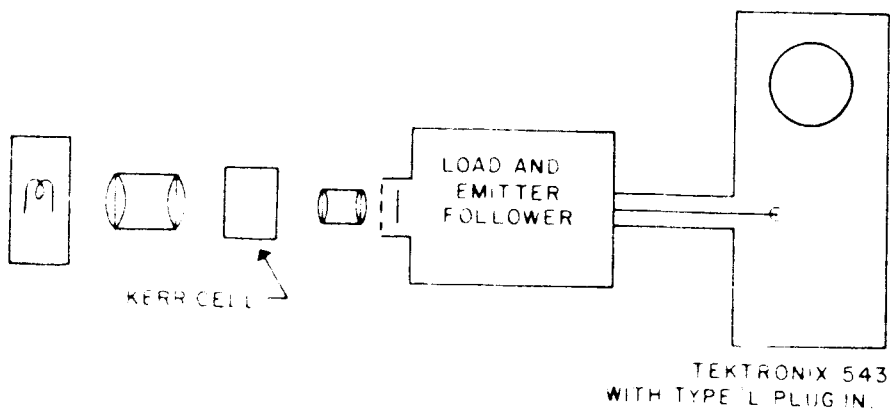


FIG. 9  
DIAGRAM OF TEST SETUP

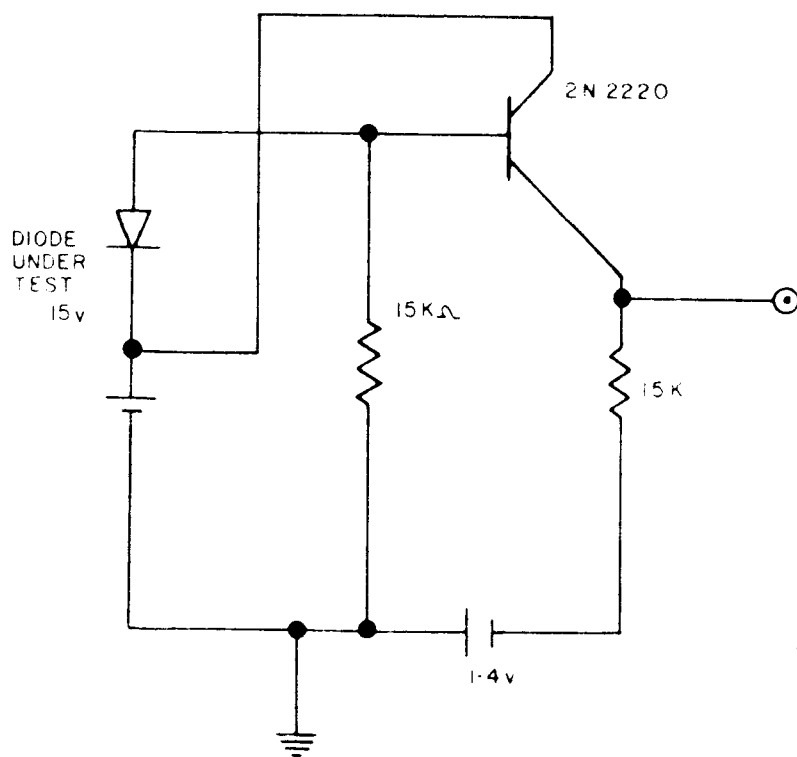


FIG. 10  
DIODE TEST CIRCUIT

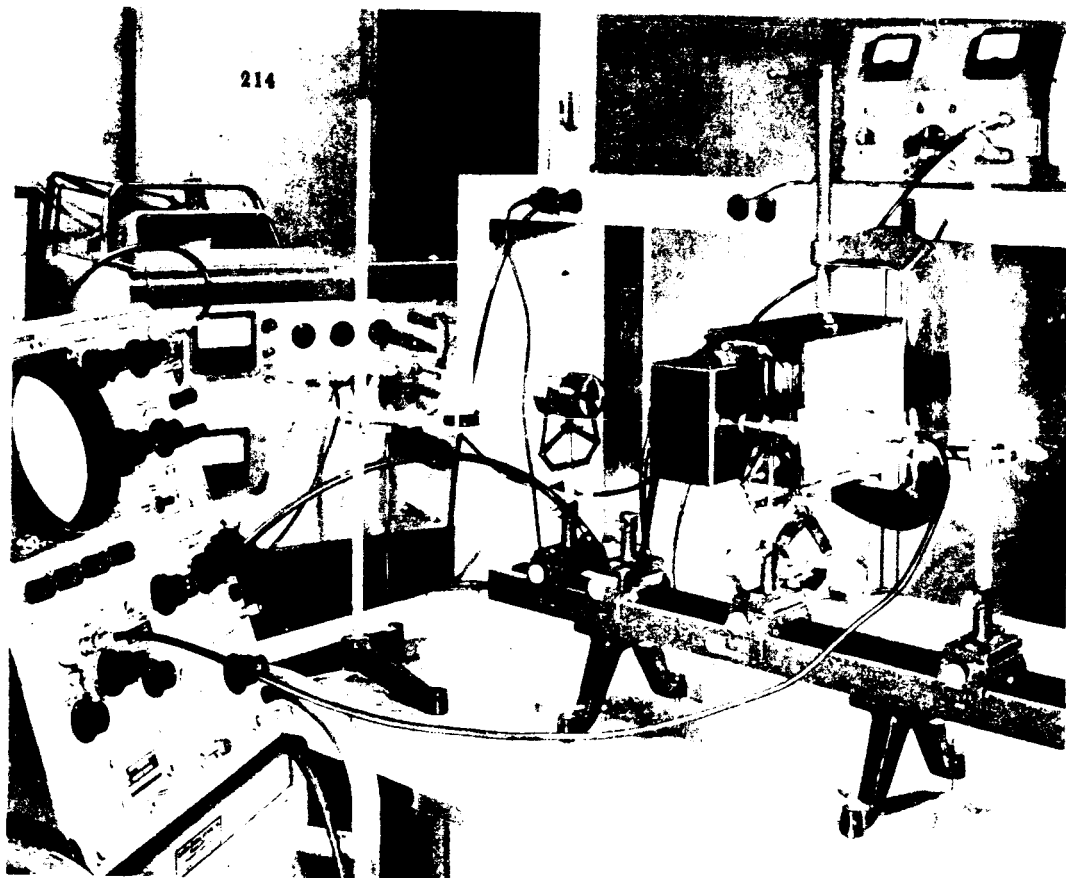
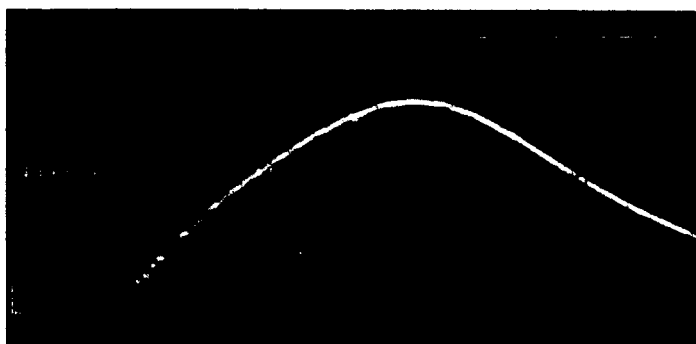
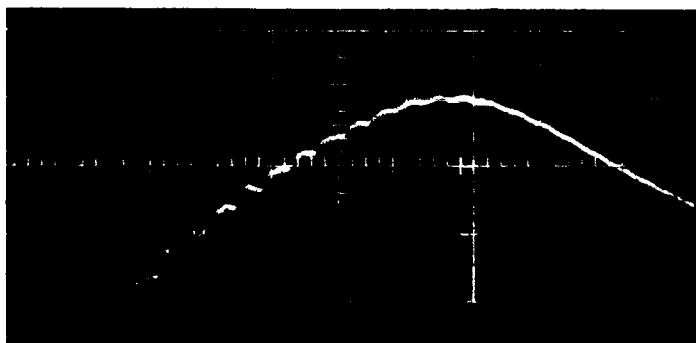


FIG. 11 TEST SETUP



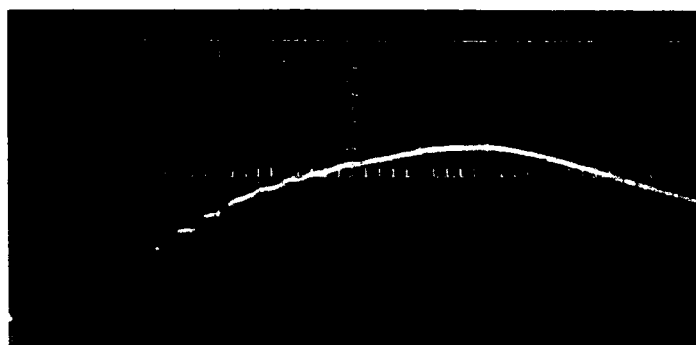
Vertical  $\times .05$  volts/division  
Horizontal  $.2 \mu\text{s}/\text{division}$

FIG. 12 GRADED BASE CELL ILLUMINATED FROM FRONT



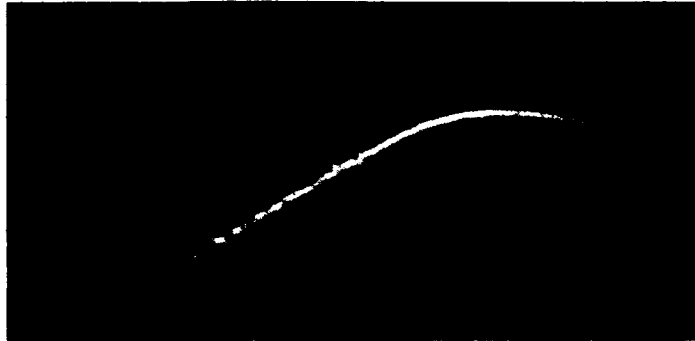
Vertical  $.05$  volts/division  
Horizontal  $.02 \mu\text{s}/\text{division}$

FIG. 13 GRADED BASE CELL ILLUMINATED FROM BACK (Unfiltered light)



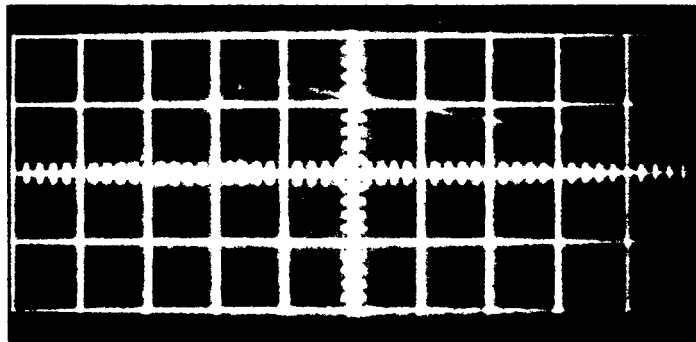
Vertical  $.005$  volts/division  
Horizontal  $0.2 \mu\text{s}/\text{division}$

FIG. 14 GRADED BASE CELL ILLUMINATED FROM BACK (Filtered light)



Vertical 0.2 volts/division  
Horizontal 0.2  $\mu$ s/division

FIG. 15 CONTROL CELL ILLUMINATED FROM  
FRONT (Unfiltered light)



Vertical .02 volts/division  
Horizontal 0.5  $\mu$ s/division

FIG. 16 CONTROL CELL ILLUMINATED FROM  
BACK (Unfiltered light)

It will also be seen that the time required for the output voltage to reach its maximum value is independent of whether the cell is illuminated from the front or the back. It may be concluded that the measurement was not sufficiently sensitive to detect the transit time difference between back and front on the graded base cell.

Figures 15 and 16 show the results of a similar experiment carried out on a specimen from a control or uniform base cell. In this case it will be seen that when illuminated from the front, the characteristics are similar to those of the graded base cell. However, when this cell was illuminated from the back, the peak of the response occurred .5 to .6 microseconds later than in the case of front illumination. The peak occurred approximately 2 microseconds after the commencement of the pulse. This is a somewhat shorter time than would be expected from the elementary theory which shows that for electrons in a layer of p-type silicon 100 microns thick, this transit time is 2.6 microseconds. Nevertheless, there is a clear difference in behavior between the graded base and the control cell, and this difference can be accounted for by assuming that there is in fact an electric field having a value between 10 and 20 volts/cm in the base region of the graded base cell. The measurements were not sufficiently precise to enable a more accurate determination to be made.

### 3.4 Cell Efficiency Measurements (Ref. 6)

Initial cell efficiency measurements were made using sunlight. The cell to be tested was mounted in a jig having a collimating tube. This test jig was mounted together with an Eppley total incidence pyroheliometer onto a platform which could be manually tracked to follow the sun. The pyroheliometer was also fitted with a collimating tube, and the solid angles subtended by both tubes were the same. The output voltage and output current were measured on an X-Y recorder. The output voltage was measured directly and the output current was measured by recording the voltage drop across a 1 ohm resistor placed in series

with the cell. A complete V-I characteristic was plotted for each cell while the sun intensity was measured using the pyrheliometer and an L and N potentiometer. One group of 45 cells had its V-I characteristics measured in the Electro-Optical Systems parking lot and on Table Mountain. In the parking lot the following results were obtained. 15 had efficiencies less than 9 percent, 22 had efficiencies between 9 and 10 percent, and 12 had efficiencies greater than 10 percent. Of these cells 9 were p-on-n having efficiencies in the 9 to 11 percent range. These cells were taken to Table Mountain and their efficiencies were measured on the 2nd of October. The average of the efficiencies measured in the parking lot exceeded the average of those measured on the mountain by .027 percent. The standard error of this mean value was calculated and found to be .08 percent. Applying a student t-test a t value equal to .003 was found. This difference in mean values was therefore not significantly different from zero.

When carrying out irradiation tests, it was not convenient to use sunlight. The cells therefore, were alternately bombarded with high energy particles and measured in a set up, using tungsten illumination having a 2800°K color temperature. The incident illumination was not filtered. The cells were kept at room temperature by circulating air past them. The V-I characteristics were then plotted for each cell.



## 4. THEORY

### 4.1 Introduction

In the following sections the results of detailed calculations on the collection of minority carriers from the base region of a solar cell are presented. In these calculations we have presented the collection efficiency from the base as a function of diffusion length for various distributions of the electric field within the base. The calculations were carried out both for sunlight and 2800°K tungsten illumination.

Due to the non-analytic nature of both the solar spectrum and the spectral absorption of silicon, it was necessary to solve the equations numerically and this was done on an IBM 1620 computer.

Appendix I lists the Fortran programs which were used.

The results are presented in graphical form herein.

### 4.2 Continuity Equation

The collection efficiency of a semiconductor junction device with a built-in field is usually calculated from the continuity equation (Ref. 7). For a one dimensional current flow, the steady state current flow equations are:

$$\frac{dJ_n}{dx} - e(R-G)=0; \quad \frac{dJ_p}{dx} + e(R-G)=0 \quad (4a, 4b)$$

$$J_n = e \left( n \mu_n E + D_n \frac{dn}{dx} \right); \quad J_p = e \left( p \mu_p E - D_p \frac{dp}{dx} \right) \quad (5a, 5b)$$

$$J_{Tot} = J_n + J_p; \quad J(n=0)=0 \quad (6)$$

$R$  = recombination rate  
 $G$  = generation rate  
 $n$  = added electron concentration  
 $p$  = added hole concentration  
 $n = p$  for optically generated carriers

In an n-on-p junction device the current is given by

$$J_{\text{Tot}} = e \left( D_n \frac{dn}{dx} \Big|_{x=a_+} + D_p \frac{dp}{dx} \Big|_{x=a_-} \right)$$

Where the terms on the right side represent the total current generated below and above the junction, respectively, and the junction is placed at  $x = a$ .

The total collection efficiency is given by

$$Q_{\text{Tot}} = \frac{J_{\text{Tot}}}{J_{\text{Tot}} + \int_0^{\infty} e N(x) dx} \quad (7)$$

where  $N(x) = G$  is the concentration of absorbed photons and the back surface of the device is at  $x=b$ .

The collection efficiency below the junction is given by

$$Q_2 = \frac{D_n \frac{dn}{dx} \Big|_{x=a_+}}{D_n \frac{dn}{dx} \Big|_{x=a_+} + \int_0^{\infty} N(x) dx} \quad (7a)$$

and  $Q_{\text{Tot}} = Q_1 + Q_2$

To solve for  $J$ , equations 1 and 2 are combined.  $G$  is given by  $\int_0^{\infty} G N(\lambda) \alpha(\lambda) e^{-\alpha x} d\lambda$  where  $\lambda_G$  is the wavelength corresponding to the energy gap of the material. For silicon,  $\lambda_G$  is approximately 1.11 microns.  $R$ , the recombination rate, depends on the added carrier concentration. For  $n \ll n_0$ ,  $n \ll p_0$ ,  $n_0 \ll p_0$ ,  $R = n/\tau_n$ . The

result is the continuity equation

$$\frac{d}{dx} (n\mu_n E + D_n \frac{dn}{dx}) - \frac{n}{\tau_n} + \int_0^{\lambda_G} N(\lambda) \alpha(\lambda) e^{-\alpha x} dx = 0 \quad (8)$$

For the case of a small constant field

$$D_n \frac{d^2 n}{dx^2} + \mu_n E \frac{dn}{dx} - \frac{n}{\tau_n} + \int_0^{\lambda_G} N(\lambda) \alpha(\lambda) e^{-\alpha x} dx = 0 \quad (8a)$$

Equation (8a) has generally been used in the literature to represent devices with built-in fields (Ref. 8-10). However, its use necessitates the following assumptions:

1. E is constant and not affected by generated carriers.
2.  $\mu_n$ ,  $D_n$  are independent of position
3.  $n \ll n_p$

The validity of these assumptions are discussed below.

#### 4.3 Absorption Properties and Field Effects

Solar cells are tested by illuminating them with either sunlight or 2800°K tungsten light. The tungsten light is sometimes used with a water filter to cut down heating effects from the infrared. The photon spectra for these two sources are shown in Fig. 17 and the distribution of absorbed photons in silicon are shown in Figs. 18 and 19. It can be seen that sunlight will generate a greater number of carriers in the front of the cell than does tungsten light. Therefore, events which occur deep in the cell, such as radiation damage, are accentuated by tungsten light over sunlight.

From the impurity concentrations measured on actual cells, the electric field has been calculated for a base width of 125 microns

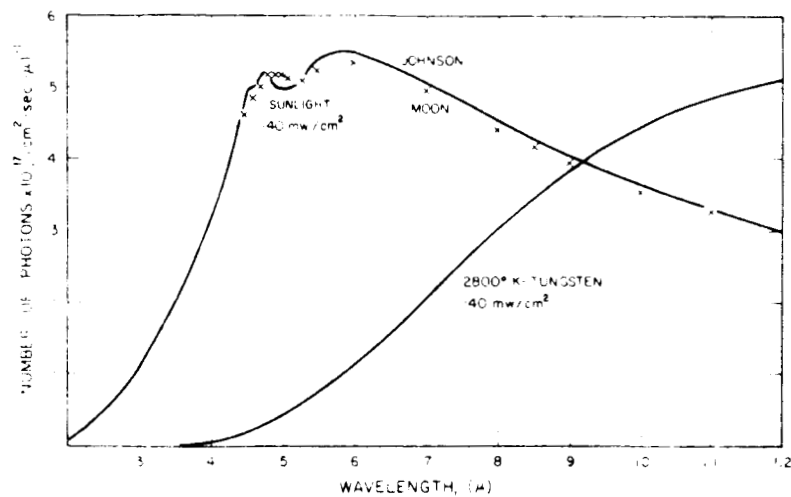


FIG. 17

PHOTON SPECTRA FOR SPACE SUNLIGHT  
AND 2800°K TUNGSTEN LIGHT

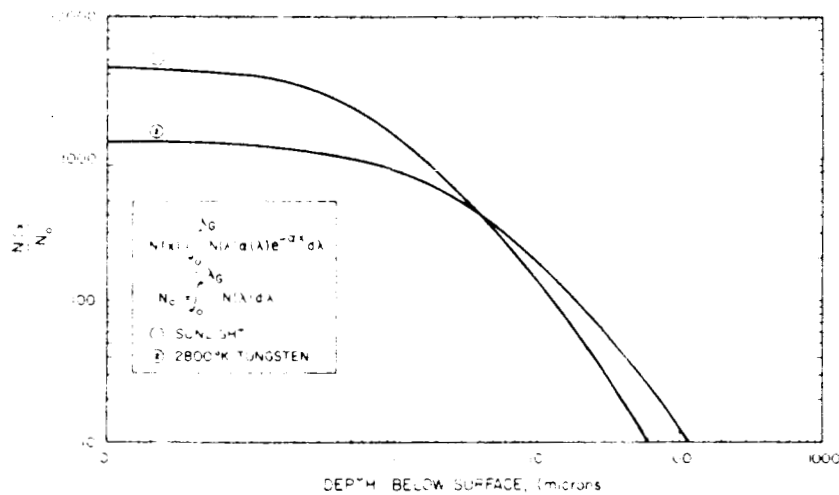


FIG. 18

ABSORPTION OF PHOTONS IN SILICON -  
DIFFERENTIAL SPECTRA

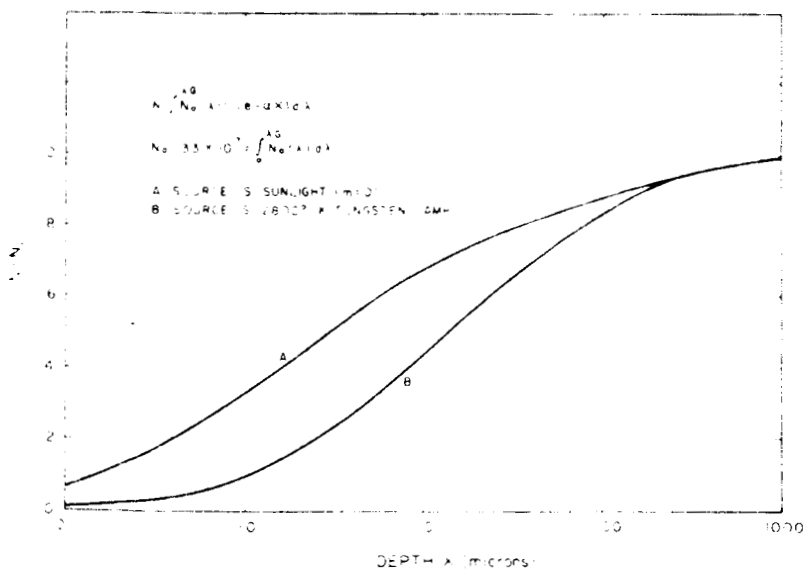


FIG. 19

NUMBER OF SOURCE PHOTONS ABSORBED  
ABOVE DEPTH X: SILICON

(Fig. 20 ). Later cells have been made with base widths of 100 microns. The distributions is very close to a complementary error function. An exponential distribution is needed to give a constant field and is actually very close to the actual distribution. For simplicity, a constant field has been assumed in all calculations.

The mobility and diffusion constant also vary with impurity concentration (Fig. 21 ). The mobility variation in a 100 micron base region is shown in Fig. 22. This actual functional relationship with position has not been included in the calculations because of the large increase in difficulty of solution. However, the error from using a constant value of  $1300 \text{ cm}^2/\text{volt-sec}$  is not large. From Figs. 21 and 22, it has been calculated that if all carriers generated in a  $100\mu$  base were collected, the average mobility of solar generated carriers would be  $1260 \text{ cm}^2/\text{volt-sec}$  and of tungsten generated carriers,  $1220 \text{ cm}^2/\text{volt-sec}$ . For an actual cell where all carriers are not collected, the ones in the back are more likely to recombine, hence the mobilities would be even closer to  $1300 \text{ cm}^2/\text{volt-sec}$ .

#### 4.4 Carrier Distribution

To test whether the solar cell operates in the small signal condition, equation ( 8a) can be solved and the results tested for consistency. The boundary conditions for an infinite base width are  $n(a)=0$  and  $n(\infty)=0$ . The results of the calculations for various values of  $E$  and  $L = (D\tau)^{1/2}$  are shown in Figs. 23 and 24. In a practical cell,  $L$  is less than 200 microns. It is seen that  $n$  is always less than  $8.2 \times 10^{12}/\text{cm}^3$ , whereas the impurity concentration varies from  $10^{14}/\text{cm}^3$  to  $10^{20}/\text{cm}^3$ . The ratio of  $n(x)/P(x)$  is always less than 0.01. Hence, the small signal assumption is valid. This means that the expression  $R = n/\tau_n$  is valid and that  $E$  is essentially independent of  $n(x)$ . It should be noticed in Fig. 24 that as  $E$

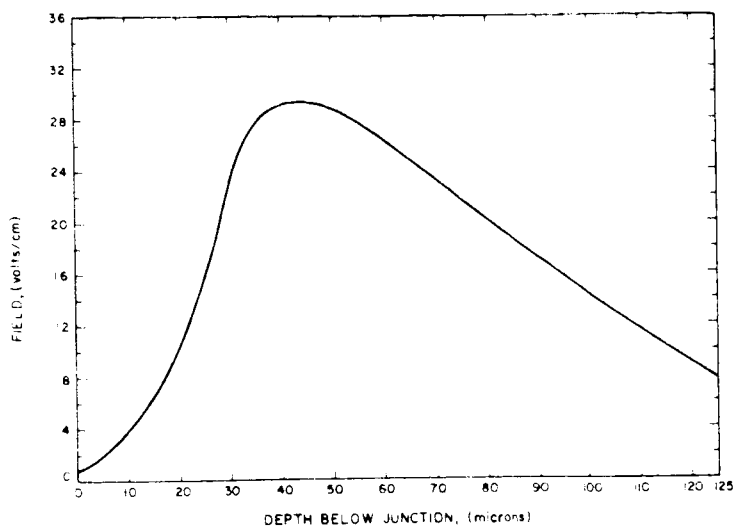


FIG. 20  
FIELD IN BASE REGION AS A  
FUNCTION OF DISTANCE FROM  
THE JUNCTION

FIG. 21  
ELECTRON MOBILITY VS IMPURITY  
CONCENTRATION IN SILICON

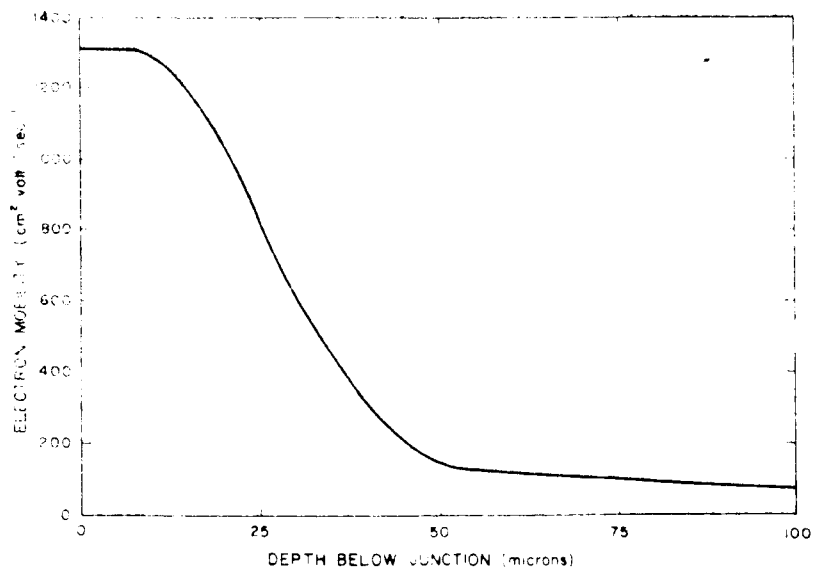
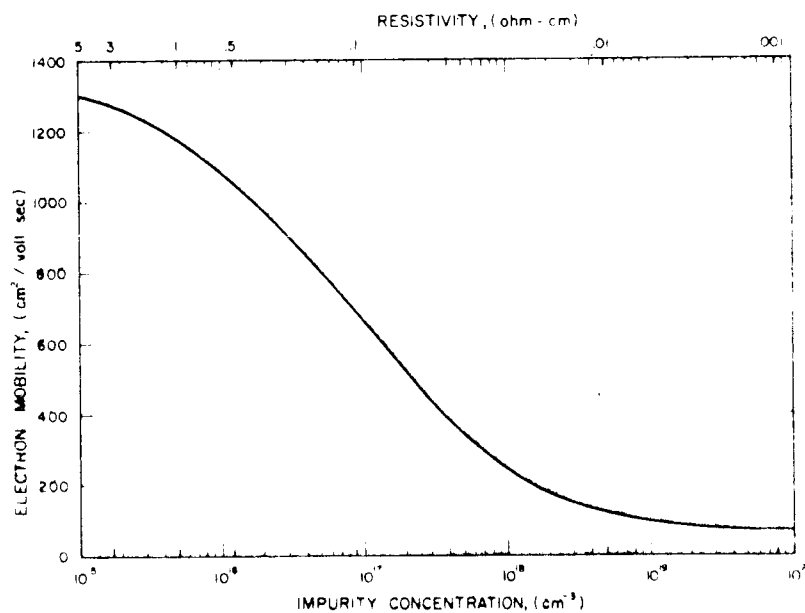


FIG. 22  
ELECTRON MOBILITY IN GRADED  
BASE SOLAR CELL

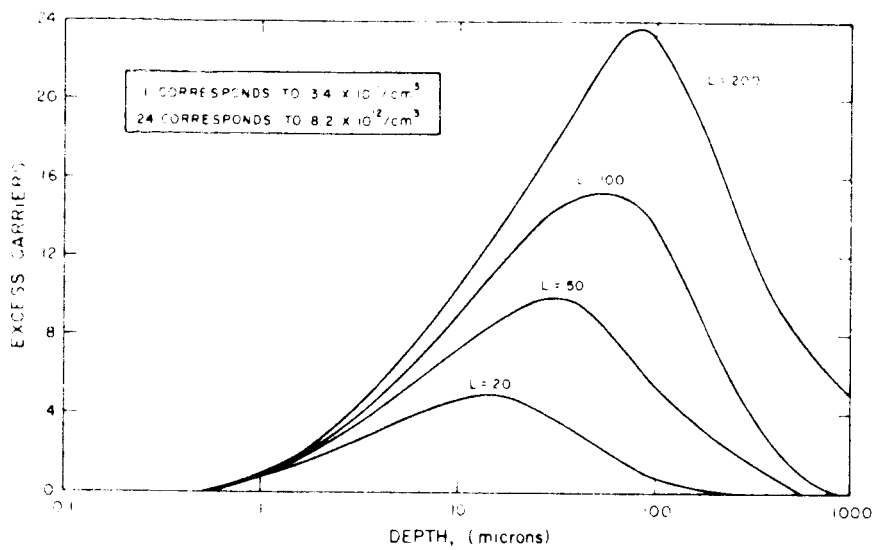


FIG. 23  
EXCESS CARRIER DISTRIBUTION  
( $E = 0$ )

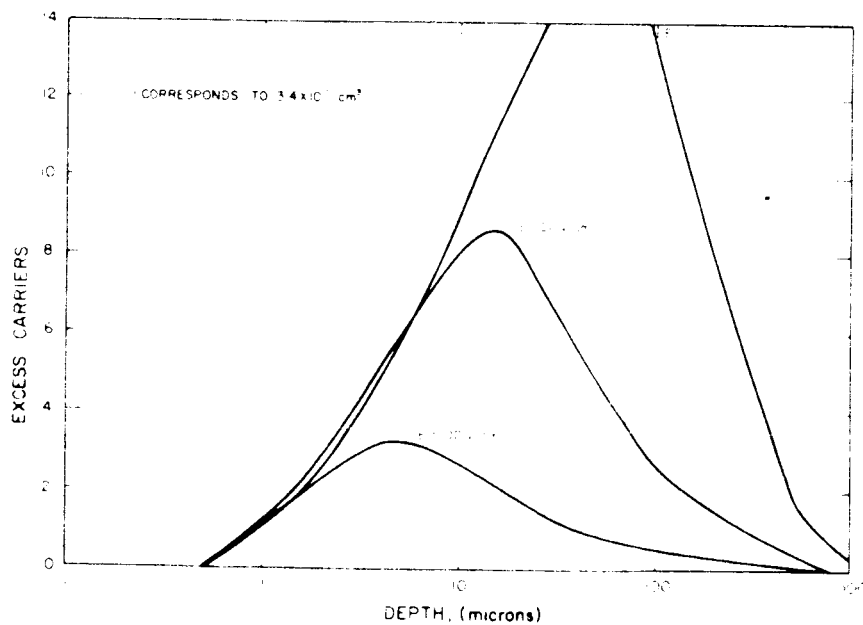


FIG. 24  
EXCESS CARRIER DISTRIBUTION  
FOR  $L = 100$  MICRONS

increases,  $n(x)$  decreases almost everywhere; this occurs because, in the steady state, more carriers are pushed across the junction by higher field strengths. Irradiation of a solar cell has the primary effect of lowering the lifetime,  $\tau$ . Since  $R = n/\tau$ , this increases the recombination rate. The addition of the field lowers  $n$  and keeps  $R$  at a low value. This can be used as a qualitative explanation of why the field causes radiation resistance.

It should be mentioned that for a solar cell with a base impurity concentration of  $10^{14}/\text{cm}^3$  near the junction, the junction width is about 3 microns. Hence, some of the carriers are generated in the depletion region.

The use of diffusion length,  $L$ , as a parameter for graded base cells may be questioned, since it is not measurable for these cells. Two arguments can be made. Firstly, the use of  $L$  as an analytic tool to show qualitative changes in short circuit current,  $I_{sc}$ , or lifetime,  $\tau$ , is valid, since exactness is not claimed. Secondly, the lifetime is a more fundamental parameter than diffusion length and  $\tau$  is meaningful in the graded-base cell. Lifetime does not change significantly with position, since the base region is extrinsic over its whole range. In this respect,  $L$  is just used to show proportional changes in  $\tau$ . The use of  $D$  (diffusion constant) as a constant is subject to the comments of  $\mu$  (mobility) above since Einstein's relation gives  $eD = KTp$ .

#### 4.5 Collection Efficiency

The collection efficiency in the base region has been calculated\* for both infinite and finite cells with widths of 100 microns and 400 microns for various values of  $E$  and  $L$ , using equation (8a). The boundary conditions are, for infinite cells,  $n(0) = 0$ ,  $n(\infty) = 0$ , and for finite cells,  $n(0) = 0$ ,  $Dn'(b) = (\mu EL + sL)n(b)$ . The back contact is at  $x = b$  and  $S$  = surface recombination velocity.

\*See equations (7) and (7a)



D is assumed to be  $30 \text{ cm}^2/\text{sec}$ . and  $S = 10^4 \text{ cm/sec}$ . The method of solution was similar to that of Kleinman (Ref. 8). Results are shown in Figs. 25, 26 and 27.

It is possible to produce from the above data, theoretical relationships of short circuit density,  $J_{sc}$ , versus electron flux. To get the relationship between diffusion length and particle flux, we use the formula derived from the Shockley-Read theory (Refs. 11 through 13).

$$\frac{1}{L^2} = \frac{1}{L_0^2} + K\phi \quad (9)$$

where  $\phi$  is particle flux and K is a constant for each material. Empirical values of K are, for 1 Mev electrons,  $1.45 \times 10^{-10}$  for 1 ohm-cm p-type silicon and  $4.75 \times 10^{-11}$  (Ref. 14) for 25 ohm-cm p-type silicon. These values yield the curves in Fig. 28. For these curves, it has been assumed that the graded base cells are 25 ohm-cm resistivity, whereas, actually they varied from .001 to 25 ohm-cm. Therefore, instead of using a constant K-factor for graded base cells, a variable one should have been used.

Theoretical curves of Q versus  $\phi$  are shown in Figs. 29 and 30. In these curves Q represents total collection efficiency from both the diffused and base regions. A 25 percent collection efficiency has been assumed for the diffused layer where 24 percent of solar photons and 5 percent of tungsten photons are absorbed for a .5 micron junction depth.

An empirical relationship between Q and the short circuit,  $J_{sc}$ , with tungsten light can be set by equating the theoretical value of Q for the uniform base cell at a flux level of  $10^{16}/\text{cm}^2$  to

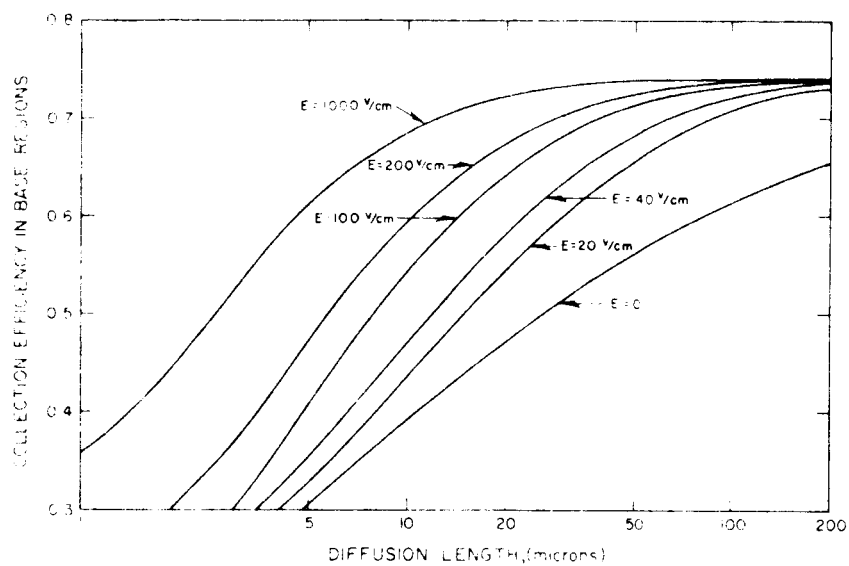


FIG. 25

COLLECTION EFFICIENCY FROM INFINITE BASE REGION VS DIFFUSION LENGTH AND FIELD STRENGTH IN SUNLIGHT

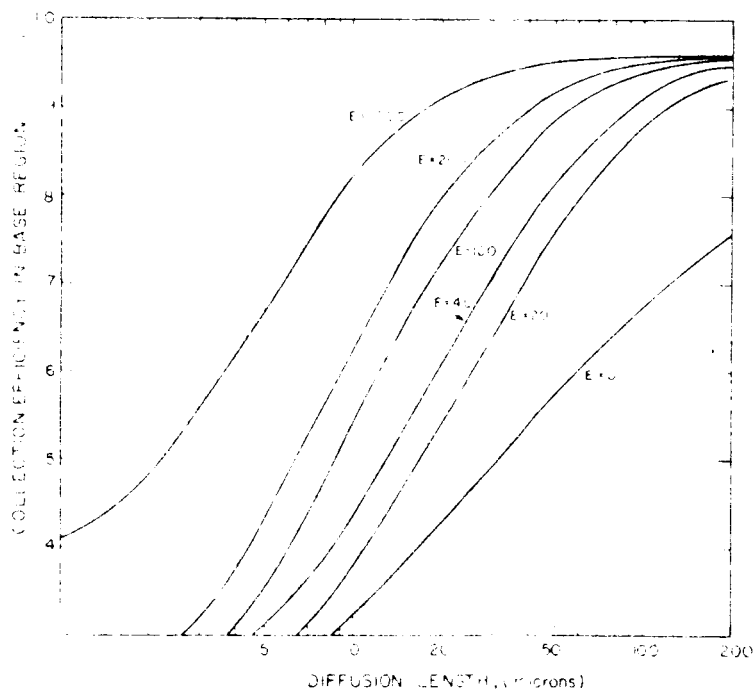


FIG. 26

COLLECTION EFFICIENCY IN 2600 Å TUNGSTEN LIGHT FROM INFINITE BASE REGION

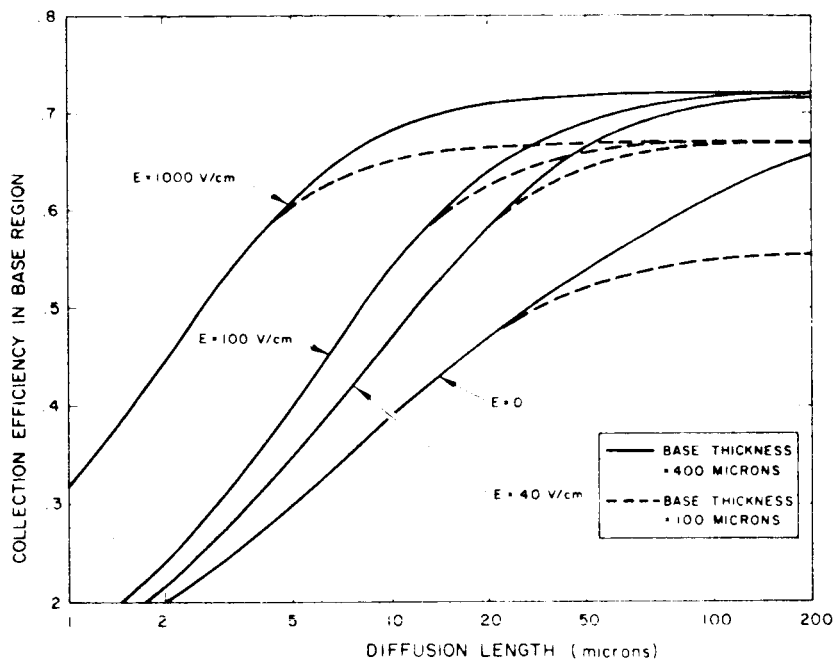


FIG. 27  
COLLECTION EFFICIENCY FOR  
FINITE BASE IN SUNLIGHT VS  
ELECTRIC FIELD STRENGTH

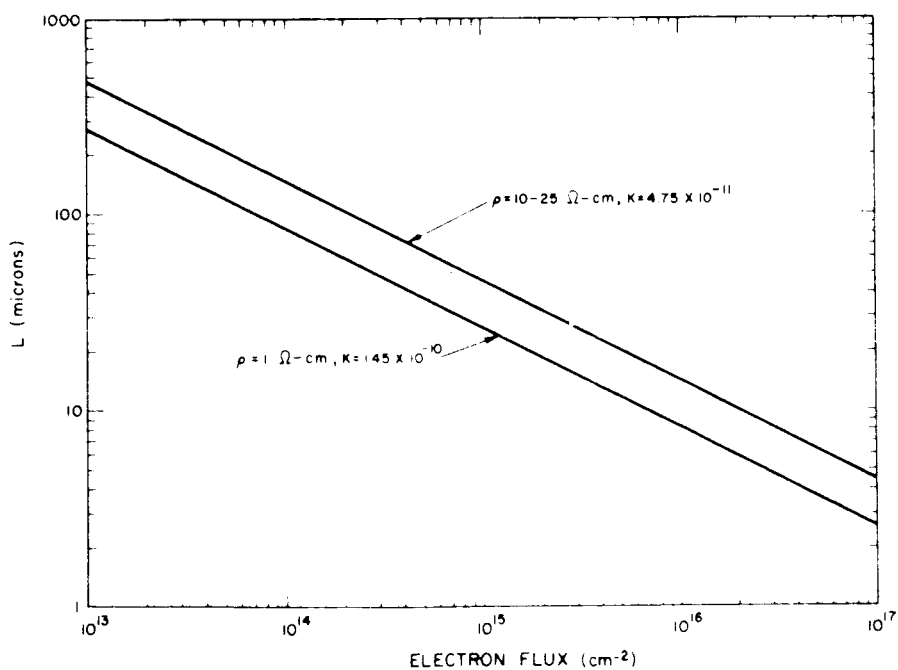


FIG. 28  
DIFFUSION LENGTH VS FLUX OF 1  
MEV ELECTRONS: P-TYPE SILICON

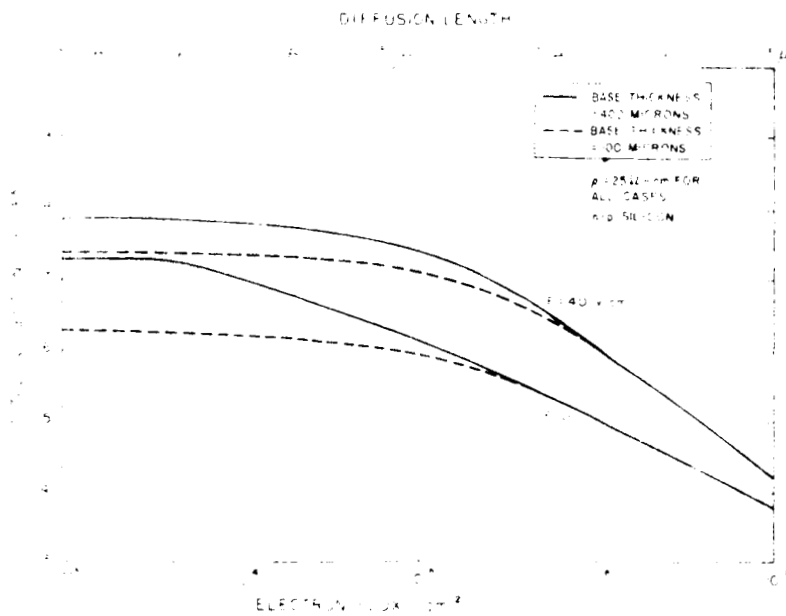


FIG. 29

TOTAL COLLECTION EFFICIENCY  
SUNLIGHT VS 1 MEV ELECTRON FLUX  
AND INTERNAL FIELD STRENGTH

FIG. 30

TOTAL COLLECTION EFFICIENCY IN  
2800°K TUNGSTEN VS 1 MEV ELECTRON  
FLUX AND INTERNAL FIELD  
STRENGTH

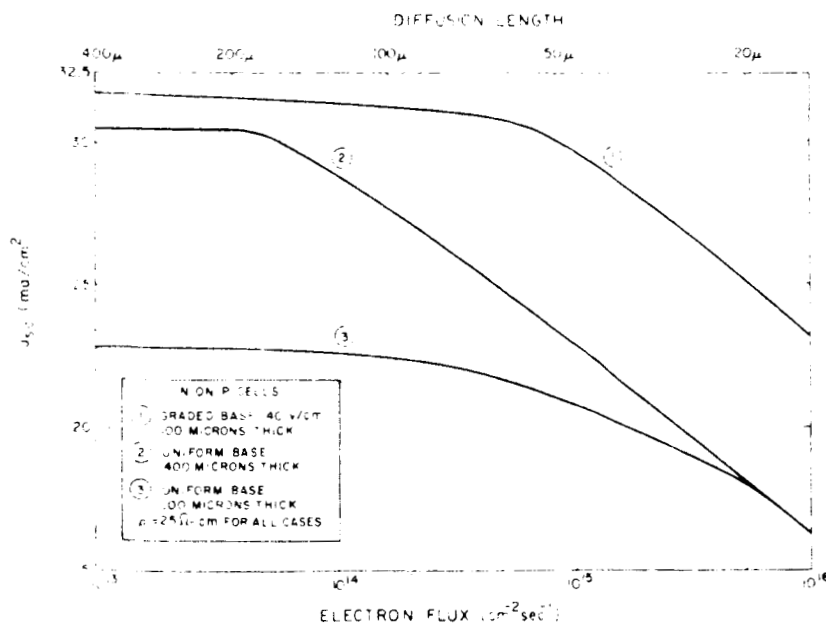
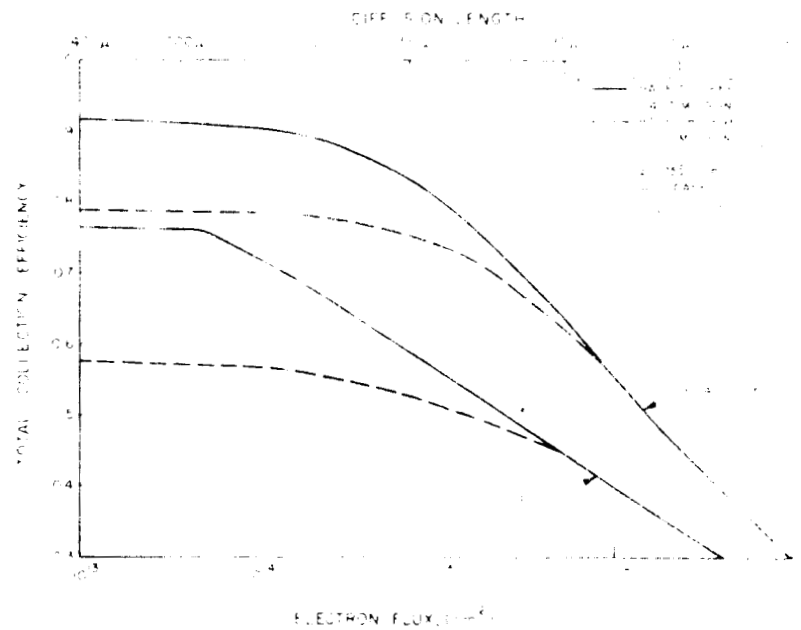


FIG. 31

THEORETICAL SHORT CIRCUIT  
CURRENT DENSITY VS 1 MEV  
ELECTRON FLUX IN TUNGSTEN  
LIGHT

the experimental value of  $J_{sc}$  for the same flux. This works out to be  $Q = 1.0$  corresponds to  $35 \text{ ma/cm}^2$ . An empirical relationship is necessary, since the exact level of light for measuring during irradiation experiments is not known. In space sunlight,  $140 \text{ mw/cm}^2$  gives  $Q = 1.0$  corresponds to  $J_{sc} = 54 \text{ ma/cm}^2$ . The curve of  $J_{sc}$  versus flux is shown in Fig. 31.

## 5. IRRADIATION EXPERIMENTS

### 5.1 Electron Irradiation

During the program five groups of n-on-p cells and one group of p-on-n cells were irradiated with 1 Mev electrons (Ref. 15 ). Figures 32 through 36 show the results obtained for the n-on-p cells. The cells were alternately irradiated and had their short circuit currents measured using unfiltered 2800°K tungsten illumination. The graphs show the short circuit current as a function of the integrated electron flux. In each case the data has been plotted on the basis of the cell having a total area of  $1 \text{ cm}^2$  with an active area of  $0.9 \text{ cm}^2$ . Figure 32 shows results obtained in two groups of control cells, that is, cells having uniform base resistivity, and is shown in overlay form for ready comparison with the results shown in Figs. 33 through 36 . The two groups of control cells were processed simultaneously on 25 ohm cm p-type silicon and differ only in the thickness of their base regions, which were 4 mils and 12 mils, respectively. At the time when these experiments were conducted there was no published data on the radiation resistance of commercial n-on-p cells which could be readily compared with the results which had been obtained on the graded base cells. Fabrication of control cells enabled us to submit samples of both uniform and graded base cells for comparative radiation studies with commercial solar cells. This enabled us to determine whether the methods of fabrication employed in making uniform case cells affected their radiation resistance compared to commercial cells. The comparative data which were obtained with commercial cells will be discussed in a subsequent section.

By examining the results shown in Fig. 32, it may be seen that the initial short circuit currents on the 12 mil thick group of control cells were considerably higher than those on the thinner cells. This is due to the fact that in the pre-irradiated condition, the diffusion length in the thin cells was comparable with the cell thickness. Thus, the collection efficiency from the base region was reduced leading to a lower short circuit current. Figure 32 clearly shows the dangers of evaluating results in terms of ratios of initial to final short circuit current. If evaluated on this basis the thin cells would show superior performance. However, it may be seen that by the time the cells have been subjected to a flux of  $5 \times 10^{15}$  electrons/cm<sup>2</sup>, the short circuit current of the two groups of cells is almost the same. Comparing the results of the control cells with the graded base cells we see that for two of the groups at an irradiation level of  $5 \times 10^{15}$ , the performance of the graded base cells was approximately the same as that of the control cells. For the other two groups it would require a factor of 2 increase in radiation to reduce the short circuit current of the graded base cells to the level reached by the control cells at the flux of  $5 \times 10^{15}$ .

It should be noted that the two groups which showed greater radiation resistance than the control cells were 4 mils thick and had the junction adjacent to the edge of the graded region.

The two groups whose performance was comparable with the controls were 4.5 mils thick and the edge of the graded region was 0.5 mils from the junction.

At the Technical Monitor's suggestion it was decided to irradiate some graded base p-on-n cells. It was felt that if these showed an improvement in radiation resistance compared with conventional p-on-n cells, a convincing demonstration of the applicability

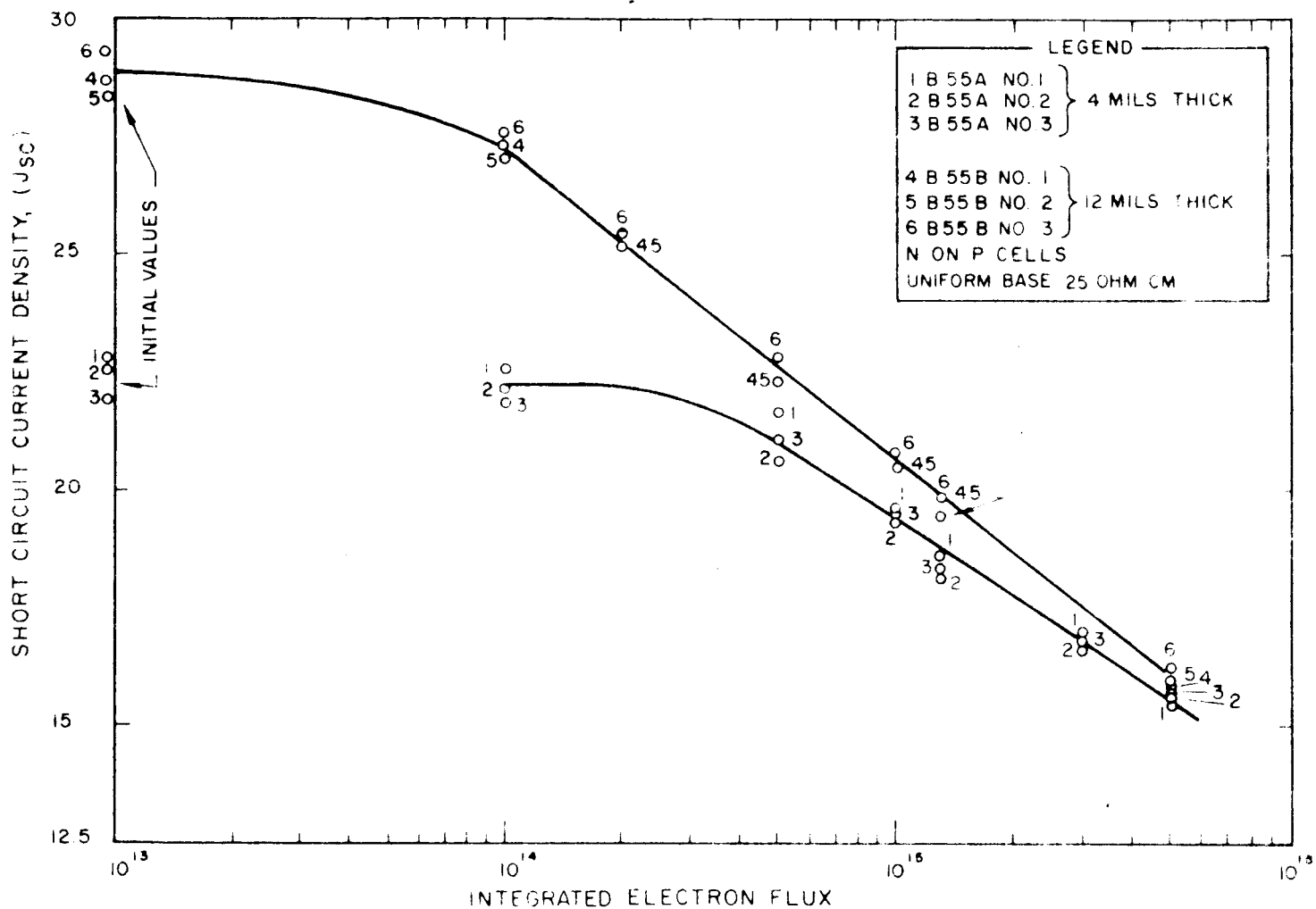


FIG. 32 SHORT CIRCUIT CURRENT DENSITY AS A FUNCTION OF 1 MEV ELECTRON FLUX



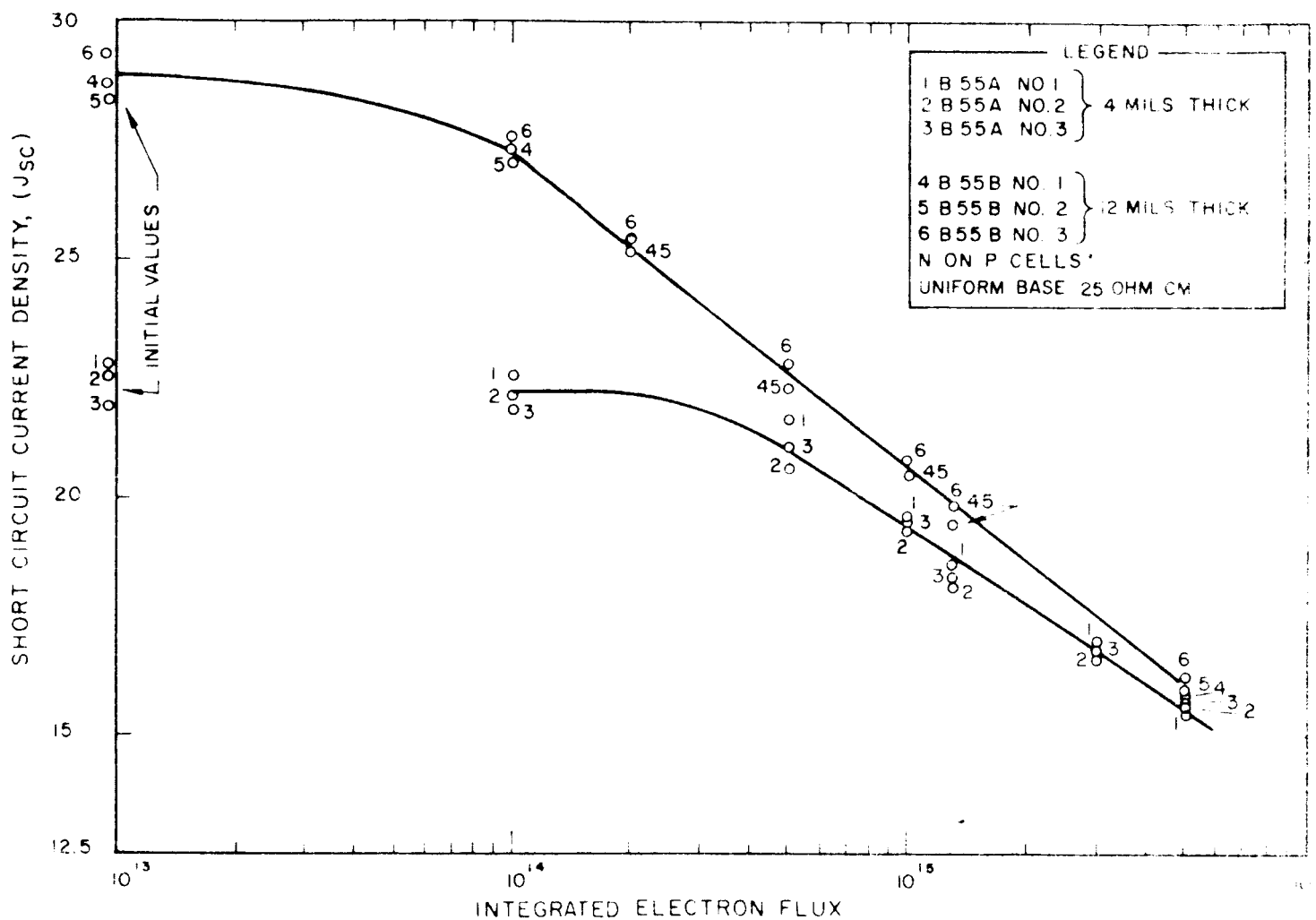


FIG. 32 SHORT CIRCUIT CURRENT DENSITY AS A FUNCTION OF 1 MEV ELECTRON FLUX

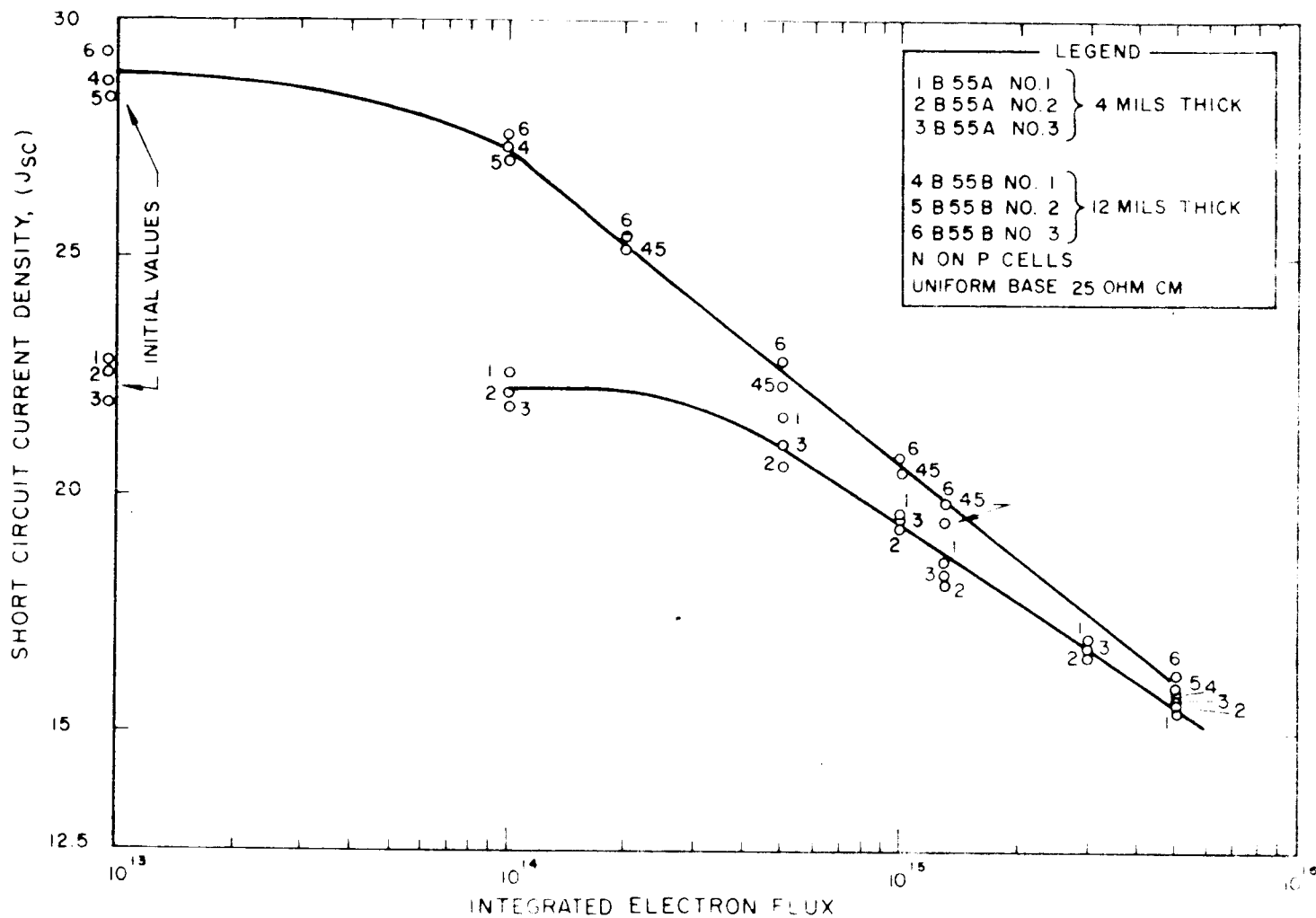


FIG. 32 SHORT CIRCUIT CURRENT DENSITY AS A FUNCTION OF 1 MEV ELECTRON FLUX

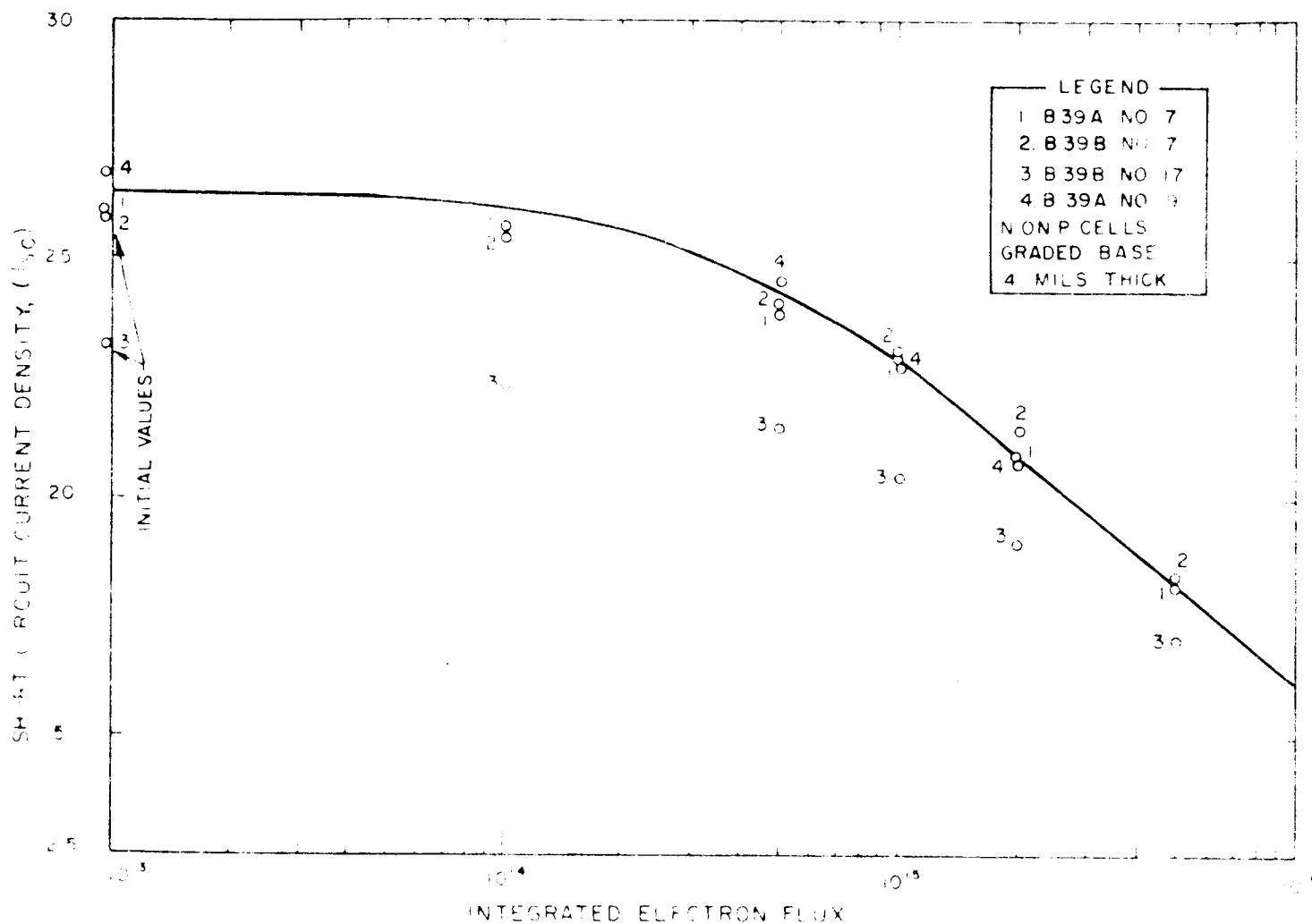


FIG. 33 SHORT CIRCUIT CURRENT DENSITY AS A FUNCTION OF 1 MEV ELECTRON FLUX

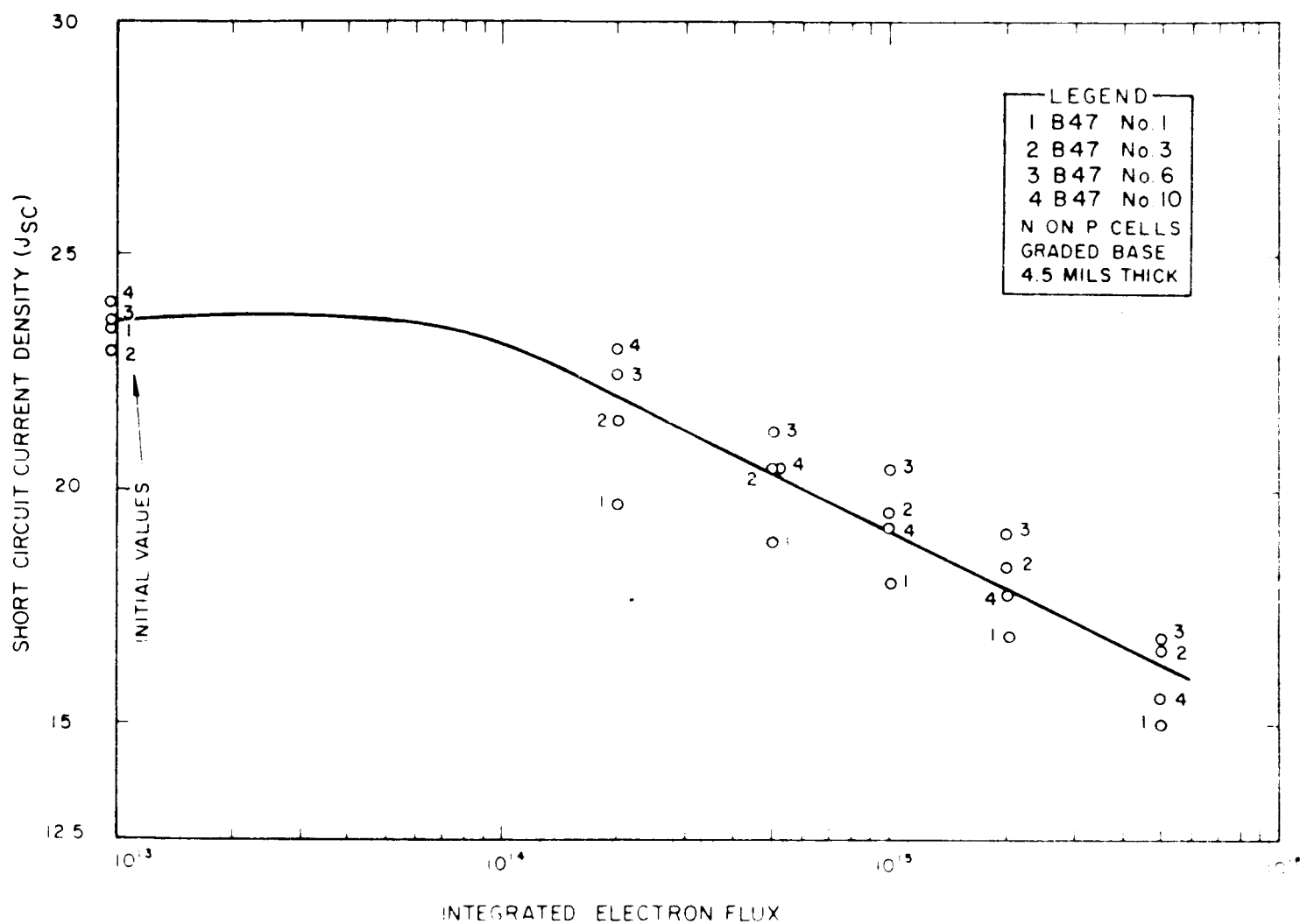


FIG. 34 SHORT CIRCUIT CURRENT DENSITY AS A FUNCTION OF 1 MEV ELECTRON FLUX

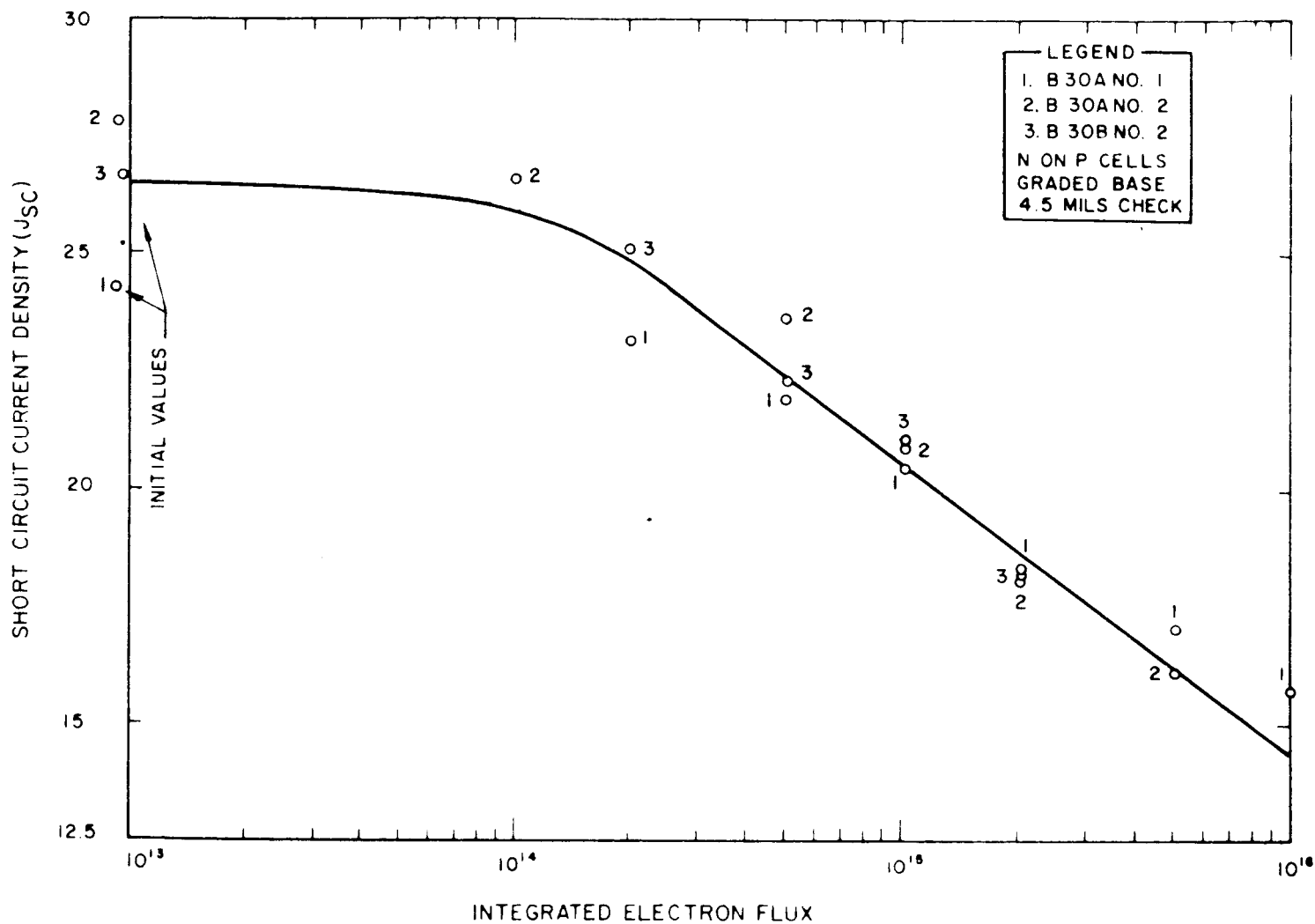


FIG. 35 SHORT CIRCUIT CURRENT DENSITY AS A FUNCTION OF 1 MEV ELECTRON FLUX



# NASA Scientific and Technical Information Facility

*operated for the National Aeronautics and Space Administration by Documentation Incorporated*

Post Office Box 33  
College Park, Md. 20740

Telephone | Area Code 301  
779-2121

PAGE NO. 46

MISSING FROM

CASE FILE DOCUMENT

N65-18448

of the graded base concept of the fabrication of radiation resistant solar cells would result. Three p-on-n graded base cells were subject to 1 Mev electron radiation in the Van de Graff accelerator at STL. The results of this experiment are shown in Fig. 37. The short circuit current of the cells when illuminated by tungsten light is plotted as a function of the integrated electron flux density; the two solid lines shown on this curve represent the performance exhibited by the majority of p-on-n commercial solar cells and the dotted line indicates the performance of the best p-on-n commercial cell. It may be observed that even though the graded base cells started off with initially smaller short circuit currents than those of typical commercial cells, these experimental cells exhibited a considerably improved radiation resistance compared with commercial p-on-n cells.

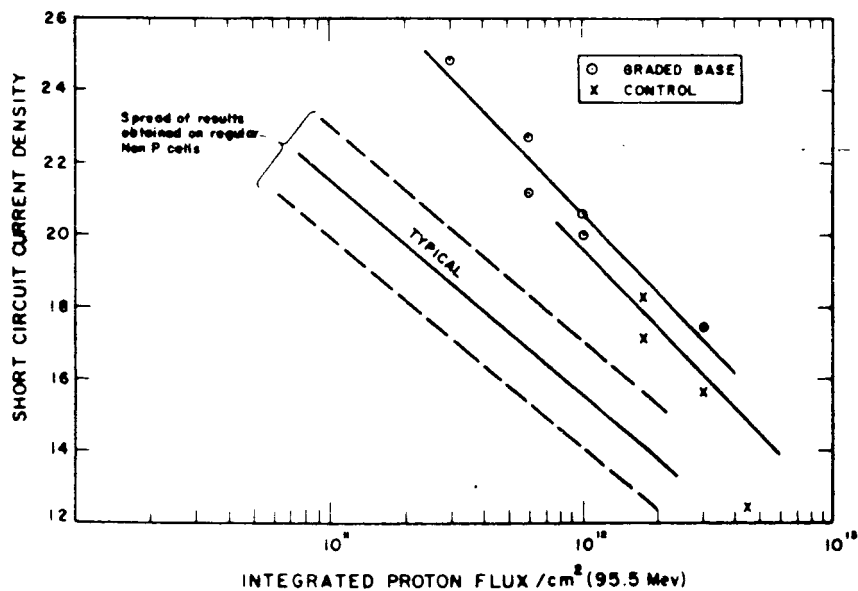
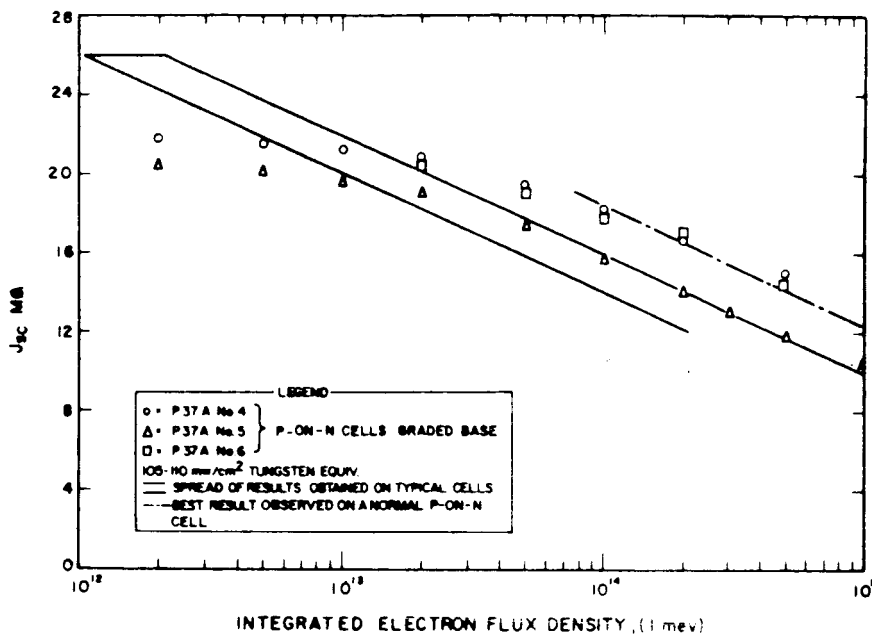
#### 5.2 Proton Irradiation

A number of n-on-p graded base and control cells were subjected to 95.5 Mev proton irradiation in the experiments carried out by Space Technology Laboratories at McGill University. The results which were obtained after recalibration of the equipment are shown in Fig. 38. It should be noted that the control cell behaved in a superior manner to cells obtained from other sources and its performance was only marginally below that of the graded base cells. It is difficult, therefore, to assess the exact significance of these results.

#### 5.3 NASA and STL Comparative Runs

Solar cells from different sources have been irradiated under identical laboratory conditions to compare their performance in a radiation environment. Experimenters at the Naval Research Laboratory under the direction of NASA and at Space Technology Laboratories each performed these experiments during the last few months. Compared were 1 ohm-cm p-on-n cells, n-on-p cells with





resistivities from 1 ohm-cm to 25 ohm-cm, and the Electro-Optical Systems' graded base cell. The results are shown in Figs. 39 and 40 . (Refs. 16 and 17.) In each case, radiation damage is lessened by increasing the resistivity of the base starting material, while the least damage occurs on the Electro-Optical Systems' graded base cell. It can be seen in the figures that although the positions of the various cells are similar in the two sets of data, the spacings are different. This is possibly due to the fact that STL used unfiltered tungsten light whereas NRL uses a water filter, changing the light spectrum. It should be noticed that the graded base cells will take 20 times more radiation than 1 ohm-cm cells and 3 times more than 25 ohm-cm cells to degrade to the same level.

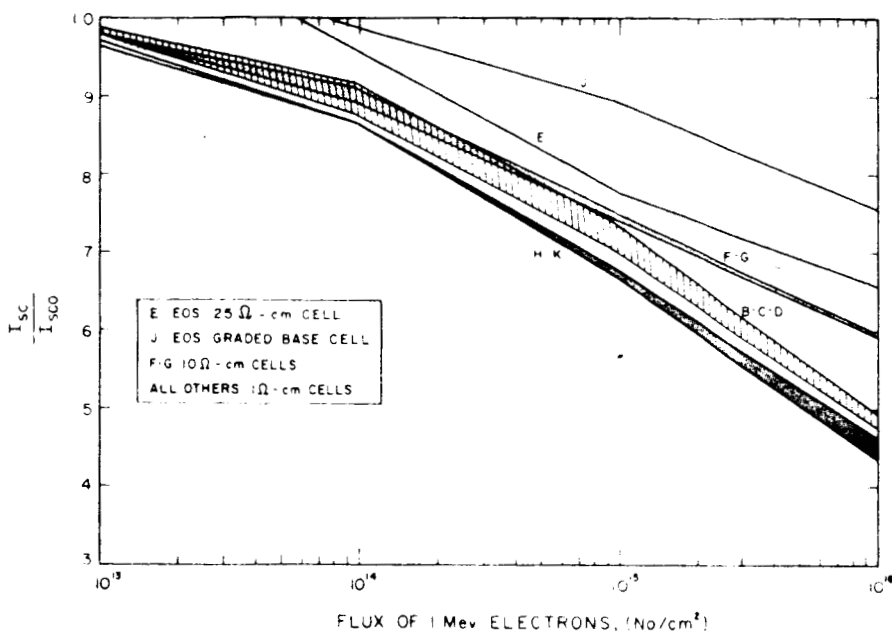


FIG. 39

COMPARATIVE DEGRADATION OF  
VARIOUS N-ON-P SOLAR CELLS  
IRRADIATED AT NRL BY NASA

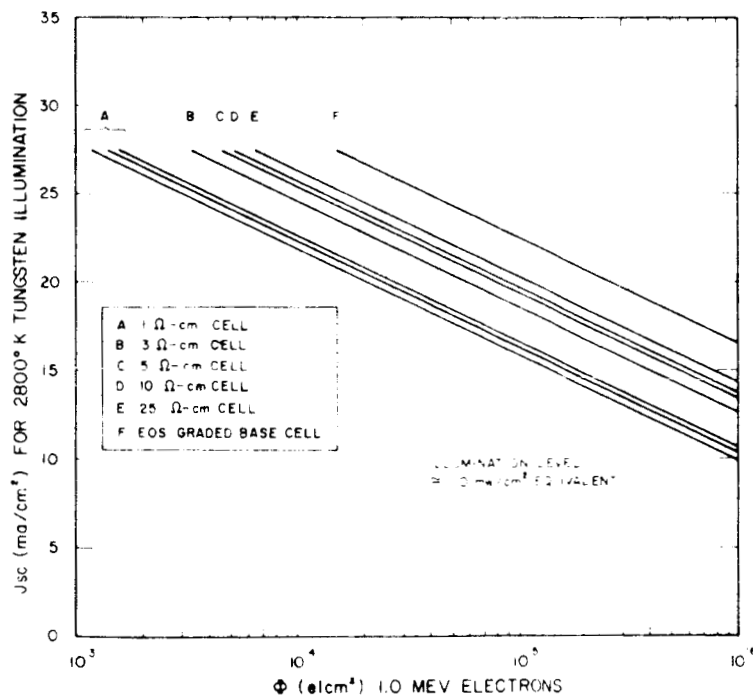


FIG. 40

COMPARATIVE DEGRADATION OF  
VARIOUS N-ON-P SOLAR CELLS  
IRRADIATED AT STL (based on  
a figure of R. G. Downing)

## 6. COMPARISON OF THEORY VERSUS EXPERIMENT

It has been conclusively demonstrated that the Electro-Optical Systems' graded base solar cell is 3 to 20 times more resistant to electron and proton irradiation than any other presently made n-on-p cell. That this property is due to the graded base structure can be seen by comparing theory with experiment. In the NASA data, Group E are Electro-Optical Systems 25 ohm-cm n-on-p cells which degraded 34.4 percent at an irradiation level of  $10^{16}$  elec/cm<sup>2</sup> measured under filtered tungsten. Theory predicts 41.3 percent degradation under unfiltered tungsten and about 10 percent less or 37 percent under filtered tungsten. For Group J, the Electro-Optical Systems' graded base cells, actual degradation was 24.6 percent. Theory predicts 26.1 percent for unfiltered tungsten and around 24 percent for filtered light. The numbers for filtered tungsten are close enough to prove the theory is reasonably correct for both graded - and uniform - base cells. Similar comparisons can be made for n-on-p cells irradiated at Space Technology Labs. Irradiations performed on p-on-n cells show that the graded base structure is again more radiation resistant, indicating that a peculiar diffusion process for n-on-p cells is not the cause of the better cells.

## 7. CONFERENCES AND PUBLICATIONS

A meeting was held on August 9th with the technical monitor at Electro-Optical Systems, Inc. Methods of fabrication of graded base cells were demonstrated and discussions took place on the progress of the program and plans were made for future work.

A meeting was held at NASA Headquarters on October 25th. Present was the technical monitor and Mr. J. Mandelkorn of NASA and Dr. M. B. Prince and Mr. S. Kaye of Electro-Optical Systems, Inc. At this time an attempt was made to see if any correlation could be obtained between this data and data obtained at other laboratories. The conclusions reached were that due to the different methods of evaluation of the cells after irradiation, it was not possible to obtain a valid comparison of data. In view of this difficulty it was decided to place more emphasis on the theoretical aspects of the work during the last part of this study.

A paper was prepared by S. Kaye, I. Weiman and W. V. Wright describing much of the work which had been done on this project. The paper was presented at the Space Power Systems Conference sponsored by the American Rocket Society which was held in Santa Monica, California from September 25 through 28th. A number of papers of interest in connection with the present work were presented at this conference. Included among these was a paper by R. Fischel of the Applied Physics Laboratory of Johns Hopkins, describing the effects observed due to the artificial radiation belt produced by the recent high altitude Johnston Island test. The effects of this

artificial radiation belt are most noticed by vehicles flying in low altitude equatorial orbits and in this case the damage rate has been increased as much as a hundredfold. A paper by J. M. Denney, STL, entitled "The Effect of Space Environment on the Photovoltaic Cell" dealt mainly with the effect of high energy proton bombardment on solar cells and the ensuing dependence on diffusion length on the incident light level. In addition to these papers a panel discussion was held to discuss the problem of radiation damage on space vehicle power supplies. The results of the panel discussions may be summarized briefly as follows: Despite the increased radiation levels arising from the artificial radiation belt, it is possible to design solar cell power systems for orbital vehicles which will be capable of operating over extended periods of time.

Mr. W. Scott visited Electro-Optical Systems, Inc., on January 31st, 1963, at which time the progress of the project was reviewed.

## 8. RECOMMENDATIONS FOR FUTURE WORK

In view of the results obtained both by NASA and ourselves in collaboration with STL, it appears that graded base solar cells offer the possibility of obtaining solar power supplies for space vehicles having considerably extended life. In order to achieve this improvement in practice we recommend that the following future work be carried out.

1. Complete calculations on the distribution of impurities in the base region required to give the optimum field distribution of the cell.
2. Fabricate these optimum structures by the use of epitaxial growth techniques for the graded base region and diffusion for junction fabrication.
3. Conduct 1 Mev electron damage and also proton damage to establish the expected performance of the optimized structures in a radiation environment.
4. Prepare preliminary cost and yield analyses of both epitaxial and diffused graded base cells.
5. On the basis of the above estimate establish a pilot line to produce sufficient cells that final estimate of yields and costs can be established.
5. Having obtained a cost estimate as a result of the pilot run, determine whether the use of these cells is economically justified for future NASA missions.

#### REFERENCES

1. EOS Progress Report for November 1961, 2080-ML-1.
2. J. Mandelkorn, et al., "A New Radiation Resistant Silicon Solar Cell", USARDL - Report 2162.
3. B. Lax and F. S. Neustadter, "Transient Response of a P-N Junction, J. Applied Physics, 259, September 1954.
4. M. Wolf and H. Rauschenbach, "Series Resistance Effects in Solar Cell Measurements", AIEE Paper CP-61-1006.
5. A. K. Jonscher, "Principles of Semiconductor Devices Operation", p. 68, Wiley, 1960.
6. "Solar Power System Calibration and Testing", Proc. Solar Working Group Conference, 27-28 February 1962, Vol. II.
7. L. B. Valdes, Physical Theory of Transistors, Chap. 7, McGraw-Hill, 1961.
8. D. A. Kleinman, "Considerations of the Solar Cell," Bell Systems, Tech. Journal, 40, 85 (1961).
9. V. K. Subashiev, "Barrier Layer Photo-Effect in P-N Junctions for an Arbitrary Generation Function", Soviet Physics, Solid State 3, 2597 (1962).
10. A. G. Jordan and A. G. Milnes, "Photo-Effect on Diffused P-N Junctions with Integral Field Gradients, IRE Trans. ED-7, 242 (1962).
11. J. M. Denney, et al., "Effect of Space Environment on Photovoltaic Cells," STL Report MR-21, 20 August 1962.
12. W. Rosenzweig, "Diffusion Length Measurement by Means of Ionizing Radiation", Bell Systems Tech. Journal, 41, 1573, September 1962.
13. J. A. Baicker and B. W. Faughnan "Radiation Induced Changes in Silicon Photovoltaic Cells", Journal of Applied Physics, 33, 3271, November 1962.



14. R. G. Downing, Private Communication.
15. J. Denney and R. G. Downing, Space Technology Labs, Engineering Mechanics Laboratory, Private Communication.
16. R. G. Downing, Private Communication.
17. W. R. Cherry, "Solar Cell Radiation Damage with 1 Mev Electrons" (unpublished).

APPENDIX I  
COMPUTER TECHNIQUES

# APPENDIX I - COMPUTER TECHNIQUES

A 10-point Gauss quadrature method was used to evaluate the solutions presented in Section 4, the approach being identical to that of Kleinman<sup>1</sup>. The calculations were performed on an IBM 1620 computer with a Fortran program. To determine whether the 10-point quadrature was of sufficient accuracy, a 16-point quadrature was used on some data and the answers varied from those previously calculated by the 10-point quadrature by 0.2 percent or less. The end points values for  $\lambda$  were  $\lambda_1 = 0.42\mu$  and  $\lambda_2 = 1.08\mu$  with  $\frac{1}{2}(\lambda_2 - \lambda_1) = .33$ . The values for the variables used are shown in Table I below.

TABLE I

$\lambda(\mu)$	0.33R	$\alpha(\text{in cm}^{-1})$	Sun $\nu(\mu^{-1})$	2800°K Tung $\nu(\mu^{-1})$
0.429	0.0220	$3.7 \times 10^4$	1.22	.084
0.465	0.0492	2.0 (4)	1.50	.158
0.526	0.0723	9.0 (3)	1.57	.348
0.607	0.0888	4.3 (3)	1.62	.728
0.701	0.0977	2.2 (3)	1.51	1.27
0.799	0.0977	1.03 (3)	1.36	1.87
0.893	0.0888	4.5 (2)	1.26	2.38
0.974	0.0723	1.56 (2)	1.12	2.69
1.035	0.0492	42.	1.05	2.88
1.071	0.0220	17.	1.02	2.97

<sup>1</sup> D.A. Kleinman, "Considerations of the Solar Cell," Bell Systems Tech. Jour. 40, 85 (1961)

The following symbols have been used:

$$\bar{N} = N(\lambda) + \int_{\lambda_1}^{\lambda_2} N(\lambda) d\lambda$$

$\alpha$  = absorption coefficient

$$\lambda_G = \lambda_2 = 1.08\mu$$

$E$  = Electric field

$$\beta = \alpha/L$$

$D$  = Diffusion constant =  $30 \text{ cm}^2/\text{sec}$

$$\epsilon = \frac{EL}{.052}$$

$$\rho = (1 + \epsilon^2)^{1/2} + \epsilon$$

$$\sigma = (1 + \epsilon^2)^{1/2} - \epsilon$$

$\gamma = a/L$  ;  $a$  = position of junction

$\eta = b/L$  ;  $b$  = position of back contact

$$S = 2\epsilon + sL/D$$

$s$  = surface recombination velocity at  $b$

$$s = 10^4 \text{ cm/sec}$$

The following equations have been used and the programs for their evaluation are given in Tables II through V.

Photon Absorption - (Table II)

$$\frac{N(0,x)}{N_0} = \int_0^{\lambda_G} v(1-e^{-\alpha x}) d\lambda \quad (1)$$

$$\frac{N(x)}{N_0} = \int_0^{\lambda_G} v\lambda(x)e^{-\alpha x} d\lambda \quad (2)$$

Carrier Distribution - Infinite Base (Table III)

$$f(x) = \frac{n(x)}{N} = \int_0^{\lambda_G} \frac{\nu}{D} \frac{L}{1 - \rho(\beta + 2\epsilon)} \left[ e^{-\beta x/L} - (1 - \rho)a/L e^{-\epsilon x/L} \right] d\lambda \quad (3)$$

Collection Efficiency - Infinite Base (Table IV)

$$Q = \int_0^{\lambda_G} \frac{\nu L (1 - \rho)}{1 - 2\epsilon\beta - \rho^2} e^{-\beta x} d\lambda \quad (4)$$

Collection Efficiency - Finite Base (Table V)

$$Q = \frac{1}{(S + \epsilon)e^{\sigma\gamma - \epsilon} - (S - \epsilon)e^{\sigma\gamma - \rho\gamma}} \int_0^{\lambda_G} \frac{\nu L}{1 - \rho(\beta + 2\epsilon)} \left[ \begin{aligned} &-(\epsilon + \rho)(S + \epsilon)e^{(\sigma - \epsilon)\gamma - \epsilon\eta} \\ &+(\epsilon + \rho)(\beta + S)e^{2\epsilon\gamma - \rho\eta} + (\beta - \rho)(S - \epsilon)e^{\sigma\gamma - (1 + \rho)\eta} \end{aligned} \right] d\lambda \quad (5)$$

[illegible]

[illegible]

TABLE IV

INFINITE BASE



TABLE V

TABLE V (Continued)

# NASA Scientific and Technical Information Facility

*operated for the National Aeronautics and Space Administration by Documentation Incorporated*

Post Office Box 33  
College Park, Md. 20740

Telephone | Area Code 301  
779-2121

PAGE NO. 4 Table 11

MISSING FROM

(not producible)

CASE FILE DOCUMENT

N65-18448

# NASA Scientific and Technical Information Facility

*operated for the National Aeronautics and Space Administration by Documentation Incorporated*

Post Office Box 33  
College Park, Md. 20740

Telephone | Area Code 301  
779-2121

PAGE NO. 5 Table III  
MISSING FROM (not producible)  
CASE FILE DOCUMENT N65-18448

# NASA Scientific and Technical Information Facility

*operated for the National Aeronautics and Space Administration by Documentation Incorporated*

Post Office Box 33  
College Park, Md. 20740

Telephone | Area Code 301  
779-2121

PAGE NO. 6

Table IV

MISSING FROM

(not producible)

CASE FILE DOCUMENT

N65-18448

# NASA Scientific and Technical Information Facility

*operated for the National Aeronautics and Space Administration by Documentation Incorporated*

Post Office Box 33  
College Park, Md. 20740

Telephone | Area Code 301  
779-2121

PAGE NO. 7

Table V

MISSING FROM

(not producible)

CASE FILE DOCUMENT

N65-18448

# NASA Scientific and Technical Information Facility

*operated for the National Aeronautics and Space Administration by Documentation Incorporated*

Post Office Box 33  
College Park, Md. 20740

Telephone | Area Code 301  
779-2121

PAGE NO. 8 Table V

MISSING FROM

(unproducable)

CASE FILE DOCUMENT

N65-18448